Review

Molecular mechanisms for generating transmembrane proton gradients ☆

CrossMark

M.R. Gunner *, Muhamed Amin, Xuyu Zhu, Jianxun Lu

Department of Physics MR-419, City College of New York, 160 Convent Ave, New York, NY 10031, USA

A B S T R A C T

Membrane proteins use the energy of light or high energy substrates to build a transmembrane proton gradient through a series of reactions leading to proton release into the lower pH compartment (P-side) and proton uptake from the higher pH compartment (N-side). This review considers how the proton affinity of the substrates, cofactors and amino acids are modified in four proteins to drive proton transfers. Bacterial reaction centers (RCs) and photosystem II (PSII) carry out redox chemistry with the species to be oxidized on the P-side while reduction occurs on the N-side of the membrane. Terminal redox cofactors are used which have pK_as that are strongly dependent on their redox state, so that protons are lost on oxidation and gained on reduction. Bacteriorhodopsin is a true proton pump. Light activation triggers *trans* to *cis* isomerization of a bound retinal. Strong electrostatic interactions within clusters of amino acids are modified by the conformational changes initiated by retinal motion leading to changes in proton affinity, driving transmembrane proton transfer. Cytochrome c oxidase (CcO) catalyzes the reduction of O_2 to water. The protons needed for chemistry are bound from the N-side. The reduction chemistry also drives proton pumping from N- to P-side. Overall, in CcO the uptake of 4 electrons to reduce O_2 transports 8 charges across the membrane, with each reduction fully coupled to removal of two protons from the N-side, the delivery of one for chemistry and transport of the other to the P-side.

© 2013 Elsevier B.V. All rights reserved.

1. Introduction

Organisms use a transmembrane electrochemical proton gradient as a key form of stored energy [1–4]. A group of transmembrane proteins generate this gradient using the energy stored in low potential reduced substrates [5–7] or light [8]. The protons then move downhill through other membrane embedded proteins, dissipating the proton gradient to do work. The gradient is primarily used to support ATP synthesis by the F_1/F_0 ATPase [9–12], but also fuels flagellar motors [13,14] and plays a role in supporting active transport of metabolites [15–17].

This review focuses on four proteins that add to the transmembrane proton gradient: bacterial reaction centers (RCs) [18–21], photosystem II (PSII) [22–26], bacteriorhodopsin [27–31] and cytochrome c oxidase (CcO) [7,32–41]. RCs, PSII and bacteriorhodopsin use light as the energy source, while CcO uses the energy liberated by the reduction of O_2 to water [42]. Proteins that generate the proton gradient can be classified into two fundamental molecular designs (Fig. 1) [7,43]. One uses redox reactions, arranging the sites that do chemistry vectorially with respect to the membrane (Fig. 2) [44]. The second is the transmembrane proton pump (Fig. 3). RCs and PSII carry out vectorial redox chemistry. Bacteriorhodopsin is a proton pump. CcO combines both mechanisms as vectorial redox chemistry leads to the reduction of O_2 and the liberated energy drives a proton pump.

1.1. Vectorial redox chemistry

In a vectorial, redox dependent system low potential substrates that are oxidized, releasing protons are placed in binding sites on the low pH (P, positive) side of the membrane while the groups that are reduced, binding protons, are near the high pH (N, negative) side (Figs. 1b,c, 2) [44–47]. There is no proton transfer through the protein from the N- to P-side of the membrane. Electrons tunnel, through a series of intermediate acceptors [48], across the protein from the electron donor on the P-side to the acceptor on the N-side. Bacterial photosynthetic reaction centers (RCs) and green plant photosystems PSI and PSII use light energy to build the proton gradient in this manner.

Building a proton gradient by vectorial electron transfer reactions requires that the reactants and products of the redox reactions have substantially different pK_as in their oxidized and reduced states (Fig. 2). In addition, their pK_as must shift across the value of the pH. Thus, the pK_a of each oxidized species must be below the pH, while the reduced species must be above the pH on the appropriate side of the membrane. If the pK_a remains above or below the pH in both
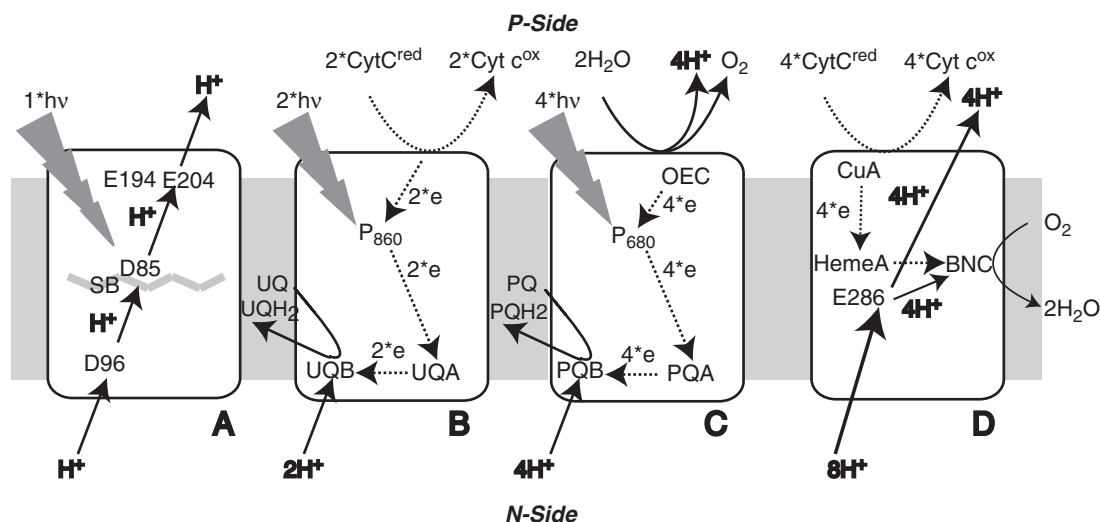
Fig. 1. Mechanisms proteins use for creating a proton gradient. Each protein removes protons from the more negative side of the membrane at high pH (N-side) and releases it on the low pH, positive side (P-side) of the membrane. Dotted lines are electron transfer reactions; solid lines are proton transfers. A. The bacteriorhodopsin proton pump. Light absorption leads to isomerization of the retinal Schiff-base (SB). Protons are transferred through the protein, but no overall chemistry is carried out. Rather, clusters of strongly interacting residues change their proton affinity when the protein conformation changes leading to a sequence of proton binding and release. The SB, D85 and D212 (not shown) make up in the central cluster (CC) and D194 and E204 form the exit cluster (EC). (B) Photosynthetic reaction centers (RCs) from purple, non-sulfur bacteria. Ubiquinone (UQ) is reduced in two light-initiated turnovers. Because the pK_a of the UQ is below 0 and that of the U QH_2 is above 10, protons are bound upon quinone reduction. The quinone, with a long hydrocarbon tail is restricted to the membrane. There is a proton pathway leading from the N-side to the quinone binding site, but no channel through the protein. The ultimate electron donor is cytochrome c, which does not require proton release to be oxidized at physiological pH. (C) Photosystem II (PSII) reduces plastoquinone (PQ) in a reaction that is analogous to that found in RCs. Water is the ultimate electron donor and it releases protons when it is oxidized to O_2 in the oxygen evolving complex (OEC) on the P-side of the membrane. There are proton pathways that connect the N-side compartment to the quinone binding site and the P-side to the OEC but none that lead across the protein. (D) Cytochrome c oxidase (CcO) reduces O_2 to water. This protein binds 4 protons from the N-side of the protein to do chemistry. At the same time 4 additional protons are pumped across the protein. The bi-nuclear center (BNC) is made up of Heme a_3, CuB and Y288. Eight protons are taken up from the N-side via the K and D channels (only one shown). E286 is a Glu with a high pK_a that sits at the top of the D channel for proton uptake.

oxidized and reduced states, there will be no proton binding or release even if there is a large change in the pK_a [49].

Vectorial redox chemistry relies on electron tunneling through the protein. Tunneling steps of 8–10 Å are optimal so the transmembrane region needs one or two intermediary cofactors to serve as stepping stones across the membrane [48,50]. The reduction chemistry of these bridging redox cofactors is usually not coupled to proton transfer. In principle, conformational changes are not required to carry out these long-range electron transfers and many of these reactions will occur in frozen samples [51–53]. While these proteins do not have transmembrane proton pathways, they will have short pathways providing access to transfer protons from the surface to the terminal electron donors and acceptors [20,54,55].

1.2. The proton pump

The other basic protein design that generates a transmembrane gradient is the proton pump. Here protons are moved through the protein from the high to the low pH side of the membrane. A pump relies on a network of proton carriers, including waters, cofactors and protonatable amino acids to ferry the proton through the protein [28,56,57]. During the reaction cycle the protein changes the thermodynamics and kinetics of proton transfers between key residues [58,59]. These changes ensure that the correct flow of protons is thermodynamically favorable in each segment of the reaction cycle and is unidirectional overall. Bacteriorhodopsin is a light driven protein that uses this mechanism [28]. Cytochrome c oxidase (CcO) is an example of a protein that carries out vectorial proton binding driven by the exergonic chemistry of oxygen reduction, which fuels a classic proton pump [6,7,32].

It is easier to design a system where the gradient is built by putting the electron donors and acceptors on opposite sides of the

membrane than to make a proton pump. Proton pumps need routes to transfer protons across the protein. These pathways are not special cofactors but simply protein side chains and internal waters whose properties are modulated through the reaction cycle. The
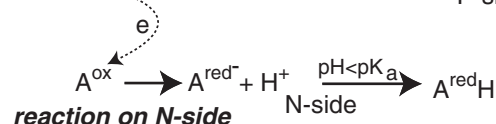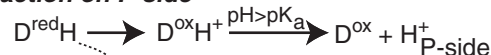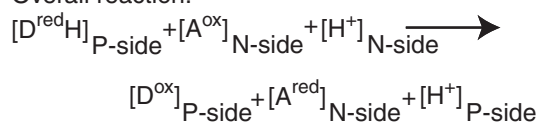

Fig. 2. The basic mechanism for vectorial proton transfer. The electron donor (D) is placed on the P-side and the electron acceptor (A) is on the N-side of the membrane. D is initially reduced and its pK_a is above the pH found on the P-side so it is protonated. When oxidized, its pK_a shifts to be below the pH on the P-side and the proton is released to the P-side. The electron tunnels across the membrane and reduces A. When A is oxidized its pK_a is lower than the pH on the N-side, however the pK_a of the reduced A^- is above the pH and it binds a proton from the N-side. As long as there is no proton transfer pathway across the membrane the proton released as $D^{red}H$ is oxidized to the P-side (lowering the pH) and the proton bound as A^{ox} is reduced from the N-side (raising the pH). The sequence here shows ET (electron transfer) preceding PT (proton transfer) (ET PT). The mechanism can be PT ET, changing the protonation state before electron transfer or can be by strongly proton coupled electron transfer (PCET) where the two processes occur in a concerted manner.
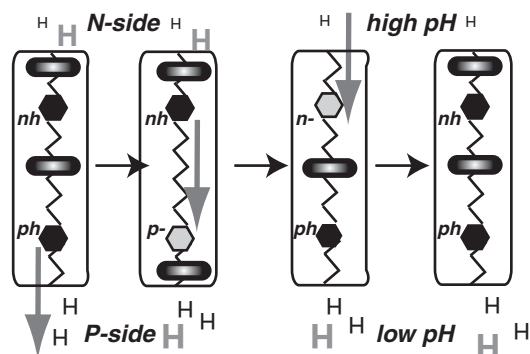
Fig. 3. A proton pump design. The simple proton pump has 2 protonable groups (n and p) and goes through 3 steps to move a proton across the membrane from the N- to P-side. The black filled hexagons have a proton (nh and ph) while the gray filled hexagons are deprotonated (n⁻ and p⁻). The ovals represent kinetic barriers for proton transfer. Initially both sites are protonated (nh, ph). In the first step the pK_a of p becomes lower than the pH so it releases a proton to form p⁻. Proton transfer across the protein is blocked so the proton adds to the proton gradient on the P-side. In the second step the pK_a of n becomes lower than p so a proton is transferred from n to p. The system moves from the (nh and p⁻) state to the (n⁻ and ph) state. The exit and entrance pathways are blocked so this is intra-protein proton transfer. In the last step the pK_a of n becomes higher than the pH on the N-side so n binds a proton. The proton transfer across the protein is blocked so the proton is bound from the N-side, resetting the system in the initial state. The order of the three steps can vary. n and p can be acidic or basic amino acid side chains or ligands.

protein passes through a set of reaction intermediates with different protonation states, driven by a series of conformational or redox shifts that change the pK_a of the key residues. It is possible in well-studied pumps such as bacteriorhodopsin to observe distinct protonation intermediates [27,30,60]. The ability to trap these states indicates they are metastable in a thermodynamic landscape that changes in an ordered way through the reaction cycle. The kinetic barriers for proton transfer must also be changing. Thus, in reaction steps where protons are bound the pathways to the N-side are open, while the connection to the P-side, where there are more protons, needs to be closed. In the steps where protons are released the pathways to the P-side are favored. Within the reaction cycle there are also steps where internal channels are open but those to the solution are not.

1.3. Modifying site proton affinities through the reaction cycle

Generating a proton gradient by either vectorial chemistry or by proton pumping requires significant changes in the proton affinity of ligands and amino acids through their reaction cycle. The ways to accomplish the pK_a changes can be separated into three basic mechanisms for discussion. One is that redox reactions substantially change the pK_a of redox cofactor serving as the electron donor or acceptor (Fig. 2). The second mechanism relies on strongly interacting clusters of protonatable residues in close proximity changing their conformation through the reaction cycle. In one conformation the cluster will bind a proton, while in another the proton is released [59,61,62]. The third mechanism is that changing the ionization states of a key group changes the electrostatic environment throughout the protein, shifting the protonation states of surrounding residues. In most proteins long-range electrostatic interactions allow the effects of reactions to propagate across the protein modifying the pK_as of more distant sites.

1.4. Protonation of redox active groups

Each of the proteins described here uses both amino acids as well as non-amino acid ligands as key components in the reaction

sequence. Biology uses a small number of redox cofactors and then modifies their function within specific binding sites so they can play a variety of roles. Cofactors such as quinones, flavins and the Mn based oxygen evolving complex (OEC) have protonatable groups as part of their core and so proton transfers can be tightly coupled to redox reactions. In contrast, the proporphyrin IX core of a heme is not directly protonable. Hemes have two open axial ligand positions in the first coordination shell of the metal that can be filled by side chains, usually of His or Met [63]. Hemes that carry out substrate redox chemistry have one side chain axial ligand and a free location for substrate or water, which can be protonatable. All hemes have propionic acids attached by single bonds to the porphyrin ring. While these acids are not directly coupled to the heme redox chemistry their pK_as are affected by the charge on the heme so they can be the site of proton loss coupled to heme oxidation [64–68]. Other cofactors such as chlorophylls and iron sulfur clusters, do not bind protons themselves so their redox reactions will change their charge state. Now long-range electrostatic interactions will modify the pK_as of nearby acidic or basic amino acids. It is these surrounding residues that then play active roles in proton transfer reactions [64].

This review describes how RCs and PSII use vectorial redox chemistry to add to the proton gradient. The analysis of bacteriorhodopsin will highlight the design features of a simple proton pump. RCs, PSII and bacteriorhodopsin are light activated, allowing detailed description of their reaction mechanisms. A number of high quality crystal structures frozen in different intermediate states of bacteriorhodopsin are used to highlight specific features connecting the structure and function of this protein. The structure and mechanism of CcO, a more complex system that combines features of both vectorial redox chemistry and proton pumping will be described and compared with the other better-understood systems. The focus is on the reaction thermodynamics, exploring in particular how the pK_as of active cofactors and amino acids are modulated through the reaction cycle in each protein. The choice of substrates and redox cofactors in each protein will be considered in light of the basic chemistry of water, quinones, hemes, Tyr and model metal complexes in solution.

2. Analysis of pK_as of protonatable groups in proteins

The goal of this review is to consider how proteins change the free energy of proton transfer through redox or conformational changes in transmembrane protons to generate a proton gradient. Experimental studies of isolated cofactors and model systems will be discussed in connection with each protein. The electrochemical midpoint ($E_{m,sol}$) and pK_a ($pK_{a,sol}$) in different solvents provides information about the basic chemistry of the key groups and the sensitivity of reactions to the environment [69–72]. In addition structure based simulations can be used to provide a framework to show in detail how the protein controls the thermodynamic landscape that leads to the observed reaction kinetics and thermodynamics. Simulation methodology provides a consistent, physics based language that can describe reactions within proteins qualitatively and quantitatively. A brief review of the concepts needed to consider how proteins may shift pK_as and E_ms in situ will be provided here. This material has been reviewed elsewhere (see [73–79] and references therein).

2.1. The response of the medium to charge changes

An individual proton or electron transfer reaction can modify its environment because it changes the charge of the reactant. The protein or any condensed medium will relax in response to the change, influencing the thermodynamics of the reaction by electronic polarization, local dipole rearrangement, long-range conformational changes, protonation shifts between nearby residues and proton

binding or release to or from the solvent [80]. Different simulation techniques have been developed to determine in situ pK_as and E_ms. Their strengths and weakness have been contrasted in earlier reviews [76,78]. Structure based methods differ in how they treat the response of the protein to proton or electron transfers. First principle quantum mechanical (QM) analysis determines the reaction free energy by calculating the difference between different assigned protonation and/or redox states using density functional theory (DFT) methods. These techniques treat only a small region of interest that has been extracted from the protein [81–85]. QM methods generally analyze the molecule in vacuum or in a simple, homogenous solvent using an implicit solvent model. QM/MM calculations allow the energy of the active site to be analyzed at a high level of theory while the influence of the rest of the protein is added via a classical, molecular mechanics (MM) treatment [86–89]. The QM and QM/MM methods do not rely on information about the chemistry of reference compounds and are able to incorporate the electronic polarizability of the molecule [90].

2.2. Classical simulation techniques to calculate shifts of E_ms and pK_as in proteins

There are a variety of computational techniques that use a classical picture of the protein [91–94]. These start with knowledge of the chemistry of isolated groups of interest in a reference solvent obtained by measurements or DFT analysis ($pK_{a,sol}$ or $E_{m,sol}$). The aim is to calculate how the protein modifies the free energy of protonation or redox chemistry using a classical treatment of the forces. One group of methods, such as MCCE (Multi-Conformational Continuum Electrostatics), uses Monte Carlo sampling of the many possible protonation and redox states of a protein to determine their Boltzmann distribution at a given solution pH and E_h and step in a protein reaction cycle [91–93]. Electrostatic energies are calculated with the equations of continuum electrostatic (CE), which average the effects of the dielectric response of the protein to the changes in charge that occurs on electron or proton transfers. In addition to the averaged, implicit response of the medium that is handled with the dielectric constant, additional, explicit, site-specific conformational changes of the system can also be included in CE/MM methods [91,93,95].

The strength of CE methods is that they can consider the large number of possible protonation states available to a protein, rapidly reaching the equilibrium distribution [96–98]. However, they treat the conformational changes that occur in response to the shifting charges in a relatively qualitative, course-grained manner. Standard molecular dynamics (MD) methods allow the protein to sample space freely but reactions cannot take place within the simulations. Thus, the protonation or redox states of the molecule are fixed. Newer methods let the protein sample different protonation states within a MD trajectory. These techniques still have difficulty bringing the charge and conformational distribution to equilibrium, but they are very promising [99–102].

2.3. Defining the free energy of electron and proton transfers

In the qualitative analysis presented in this review the underlying assumption is that the protonation and redox equilibria in proteins starts with the E_ms and pK_as in solution ($E_{m,sol}$ and $pK_{a,sok}$). The pK_a and E_m in the protein are different from that found in solution largely because reactant and product change their electrostatic energy terms differently when they are moved from solvent to protein [74,76,103]. The free energy of an individual electron or proton transfer at a given pH and E_h is:

$$\Delta G = mC\left(pK_{a,sol} - pH\right) + \Delta G_{protein} \tag{1a}$$

$$\Delta G = -nF\left(E_{m,sol} - E_h\right) + \Delta G_{protein} \tag{1b}$$

so for groups in the protein:

$$pK_a = pK_{a,sol} + \Delta G_{protein}/mC \tag{2a}$$

$$E_m = E_{m,sol} - \Delta G_{protein}/nF \tag{2b}$$

where m is the number of protons gained so is −1 for an acid, which loses a proton and 1 for a base that gains one in the reaction. n is the number of electrons gained and F is the Faraday Constant (23 kcal/mol); C is 1.36 kcal/mol or 58 meV at 25 °C. $\Delta G_{protein}$ is the change in the reaction free energy due to the environment of the group in the protein. The changes in $\Delta G_{protein}$ during the reaction cycle will induce the proton transfers needed to build the proton gradient. Computational methods provide a more complete, quantitative analysis. They consider reactions where electron and proton transfer reactions are coupled together so reactants and products have different numbers of both electrons and protons [43,104,105] and the common situation where multiple groups titrate together.

2.4. Shifting group proton affinity in proteins

In the CE worldview the factors that yield the $\Delta G_{protein}$ are divided into the changes in solvation energy and the introduction of pairwise interactions [76]. In the reaction in water, the solvation energy (Eq. (3) below) will stabilize the species with a larger charge, be it reactant or product [106,107]. When the reaction takes place in the protein all species loose solvation energy, but the more charged species looses the most and is thus more destabilized relative to the reaction in water. However, a protein can fully replace the stabilization of water that influences $E_{m,sol}$ and $pK_{a,sol}$ with specific charges and dipoles arranged around key residues and ligands. Thus, $\Delta G_{protein}$ has contributions from every protein backbone amide which has a dipole larger than water that can be oriented to stabilize buried charges [108] and the sizable fraction of the side chains that have charges or dipoles [109].

2.5. The role of the solvent

The simplest way to describe how a solvent or protein will effect redox and protonation reactions is by its dielectric constant (ε). The dielectric constant is a single number description of the degree to which a solvent can stabilize an introduced charge. A solvent with dipoles or charged groups that can change position will produce the largest dielectric constant. Water with a ε of 80 is a small molecule with a large dipole moment that can rearrange to stabilize any charged or dipolar solute. A solvent can also affect the reaction free energy by making specific interactions, such hydrogen bonds with the reactant or product. $E_{m,sol}$ and $pK_{a,sol}$ shifts between solvents with different hydrogen bonding capacity can highlight their importance in specific reactions. The solvent can also become entangled in the reaction. This is particularly important for redox reactions of protonatable substrates such as quinones. Thus, the electrochemistry in water is very different than found in DMSO, which also has a high dielectric constant of 47 but no protons [110–112]. The comparison between reactions in water and in DMSO can show how the cofactor might behave in a site where protons are not available or why proton transfer becomes rate limiting for the reaction to occur.

2.6. The solvation energy

In the CE analysis the dielectric constant is a single value that provides a sense of how much the medium, be it a homogeneous solvent

or a heterogeneous protein, will rearrange to stabilize a charge. The Born model provides a simple equation that can give a back of the envelope estimate of the stabilization of a charge in water and in protein [107,113]. Here the energy to transfer a sphere of radius r (in Å) and charge of q (in units of the charge on an electron) from water to another environment characterized by a different dielectric constant (ε_p) is:

$$\Delta G = -332 \left(q^2/2r \right) \left(1/\varepsilon_p - 1/80 \right) \; kcal/mol. \qquad (3)$$

The Born equation, with its dependence on the square of the charge, shows that a medium with a high dielectric constant will stabilize both anions and cations. Proteins, especially the relatively rigid transmembrane electron and proton transfer proteins, are considered to have a much lower dielectric constant than water. Values ranging from 4 to 12 appear to be reasonable for the protein interior [114–117]. Thus, in an electrostatic analysis there is a significant destabilization of a highly charged species when it is moved into the protein. This will always raise the pK_a of an acid and lower the pK_a of a base. Since the Born, solvation energy depends on the square of the charge, the desolvation penalty destabilizes both positive or negative charges. In contrast, specific protein binding sites are designed to favor either an anion or a cation, but not both, by placing hydrogen bond and ion pair partners around the binding site.

2.7. pH dependent pK_aS

The pK_a for a given residue in an environment with many protonatable groups depends on the charge state of the other groups in the protein. Thus, the pK_a and E_m are pH dependent [118]. A pK_a at a given pH (denoted $pK_a(pH)$) can be defined using the energy needed to change the charge on the group of interest at that pH. Thus:

$$pK_a(pH) = \Delta G(pH)/mC + pH \qquad (4)$$

where $\Delta G(pH)$ is the free energy of changing the protonation state of the residue of interest if all other residues are held at their equilibrium protonation states in the protein at this pH. The $pK_a(pH)$ for key groups change through the reaction cycle because they are participating in redox reactions, they are affected by nearby groups changing charge or because local conformational changes modify their environment. Site E_mS are also dependent on the pH since the thermodynamics of redox reactions depend on the protonation states of the surroundings [104]. Likewise, residue pK_as change with the E_h if groups in the protein undergo redox chemistry.
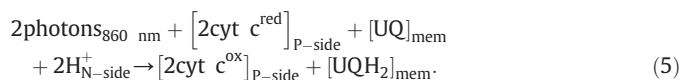
3. Mechanism of proteins that generate the proton gradient

3.1. Proton uptake to quinones at the reducing side of bacterial photosynthetic reaction centers

The photosynthetic reaction centers of purple bacteria (RCs) are well studied, light activated, proteins that contribute to the proton gradient through vectorial redox chemistry [18–20,112,119,120]. RCs and photosystem II (PSII) are Type II photosynthetic systems that release a doubly reduced quinone as a reaction product [121,122]. The quinones in RCs show how the proton gradient can be built up by keeping the cofactor near one side of the membrane in a protein without a transmembrane proton channel (Figs. 1b, 2). Thus, the quinone, a molecule where the oxidized reactant will not bind protons and the reduced product must bind them, is held on the N-side of the membrane. Many experimental [120,123–130]

and computational [61,131–136] studies have shown how RCs change the electrochemistry of the cofactor, how the surrounding protein facilitates proton uptake from solution and how the protein kinetically traps the semiquinone without making it too stable thermodynamically [136–138]. The reactions in bacterial RCs will be discussed in detail here. The reactions of the quinones on the reducing side of PSII are quite similar (Fig. 1c) [139–142].
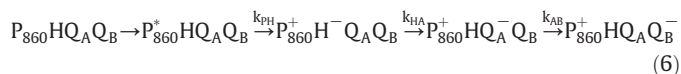
The overall reaction in RCs is (Fig. 1b):

$$2photons_{860 \; nm} + \left[2cyt \; c^{red} \right]_{P-side} + [UQ]_{mem}$$
$$+ 2H^+_{N-side} \rightarrow [2cyt \; c^{ox}]_{P-side} + [UQH_2]_{mem}. \qquad (5)$$

UQ is the oxidized ubiquinone, UQH_2 is the doubly reduced, doubly protonated product. As the quinone has a long isoprene tail it is released into the membrane not to solution. Protons are transported to the quinone binding site only from the N-side of the membrane. As there is no pathway for transmembrane proton transport, the protein does not need a mechanism to keep protons from being bound from the P-side where there are more protons. Cytochrome c (cyt c), the soluble electron donor to the RCs, is found in the periplasmic space on the P-side of the membrane. Cyt c reduction is not strongly pH dependent at physiological pH so it does not release protons as it is oxidized. There are two quinones, designated Q_A and Q_B, in RCs. In all light activated redox reactions, the photon initiates transfer of a single electron, yet the final released product is often doubly reduced. Q_A is tightly bound and is reduced only to the semiquinone, while Q_B is bound, is doubly reduced to QH_2 and released following absorption of two photons [112,120,143].

3.1.1. RC reaction sequence

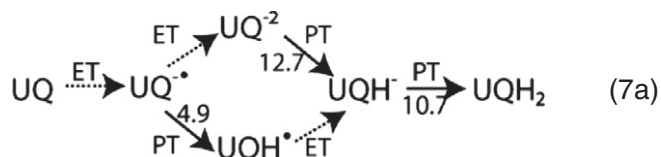The reaction following absorption of the first photon is:

$$P_{860}HQ_AQ_B \rightarrow P^*_{860}HQ_AQ_B \xrightarrow{k_{PH}} P^+_{860}H^-Q_AQ_B \xrightarrow{k_{HA}} P^+_{860}HQ_A^-Q_B \xrightarrow{k_{AB}} P^+_{860}HQ_AQ_B^-$$
$$\qquad (6)$$

where P_{860} is a dimer of bacteriochlorophylls, H is bacteropheophytin (see [144] and references therein). In RCs Q_A and Q_B are both ubiquinones. To summarize the sequence of electron transfers in RCs, absorption of an 860 nm photon excites P_{860} (Eq. (6)). Within 3 ps (k_{PH}) an electron has transferred to the nearby H, which in turn reduces Q_A, ≈25 Å from the primary donor, in ≈200 ps (k_{HA}). The reaction where H^- reduces Q_A is downhill by ≈500 meV, providing most of the driving force for the overall reaction [145]. Q_A is an example of an intermediate electron acceptor, that is not protonated when it is reduced. Nor is there significant proton binding to the protein when Q_A is reduced, as seen by the pH independence of the reaction [146–149]. There also appears to be little need for significant conformational changes within the protein to stabilize the new charge on Q_A as shown by the reaction occurring with little change in the rate of reduction down to 4 K [51–53]. At room temperature, the electron on Q_A is passed to Q_B within 100 μs (k_{AB}). This reaction is coupled to internal proton transfers and conformational changes within the protein and so it shows significant temperature dependence [150–153]. Then cyt c^{red} reduces P^+_{860} to allow a second photon to initiate a second series of electron transfers (not shown in Eq. (6)). This results in Q_B being doubly reduced, binding 2 protons and being released as QH_2.

3.1.2. Quinone redox reactions in water

It is the reactions involving Q_B that add to the proton gradient. Q_B accepts two electrons sequentially in a process that is actively modified by the protein. For any quinone going from Q to QH_2 there are 9 possible, fully oxidized, singly protonated and/or

reduced and doubly protonated and/or reduced species [110,154].[1] Some of these species have pK$_a$s that are below pH 0 (e.g. QH^{+1}, QH$_2^{+2}$, or QH$_2\bullet^+$). The instability of the protonated, oxidized quinone, QH^{+1} or QH$_2^{+2}$, is the basis of the coupling of electron and proton transfers, as it ensures the oxidized quinone will be deprotonated. Thus, 6 species are of interest here:

$$UQ \xrightarrow{ET} UQ^{\bullet-} \;\;\begin{matrix} \xrightarrow{ET} UQ^{-2} \xrightarrow[12.7]{PT} \\ \\ \xrightarrow[4.9]{PT} UQH^{\bullet-} \xrightarrow{ET} \end{matrix}\;\; UQH^- \xrightarrow[10.7]{PT} UQH_2 \qquad (7a)$$

ET indicates quinone reduction, PT indicates proton binding. The pK$_a$s for the PT reactions are associated with the appropriate arrows (Eq. 7a). In water at physiological pH, the singly reduced or protonated species are all unstable intermediates [110]. Thus, the quinone reduction reaction goes directly from Q to QH$_2$ over a wide pH range with an E$_m$ in water at pH 7 of ≈100 mV.

$$Q + 2e^- + 2H^+ \rightarrow QH_2. \qquad (7b)$$

In contrast, the semiquinone species, Q$^{\bullet-}$, is a metastable intermediate in the reactions of many proteins [155–160].

3.1.3. pK$_a$s of quinones in different redox states in solution

Measurements in mixed solvents and with analogs of the biological quinones have established the solution E$_m$s and pK$_a$s for important quinone species in solution. Knowledge of these values allow us to see how the protein modifies the reactions in situ. In water at pH 7 the low energy path for reduction of quinone to dihydroquinone (QH$_2$) proceeds through two electron transfer steps to make the semiquinone Q$^{\bullet-}$ and then Q^{-2} and terminates with two protonation steps (the top path in Eq. (7a)) [105,154]. Thus, the sequence is ET, ET, PT and PT. For ubiquinone, the semiquinone, Q$^{\bullet-}$, pK$_a$ is 4.9, while it is 12.7 for Q^{-2}, and 10.7 for the doubly reduced QH$^-$. Thus, protonating the semiquinone is uphill at physiological pH, while it is strongly favored for Q^{-2} or QH$^-$. If protons are available, the E$_m$ for reduction of the semiquinone Q$^{\bullet-}$ or QH$^{\bullet}$ is much more positive than for reduction of Q, so formation of QH$_2$ is downhill. Water plays a role in stabilizing quinone reduction even when the pH is higher than the semiquinone pK$_a$. In water above the pK$_a$ of Q^{-2}, the E$_m$ for the reduction of Q$^{\bullet-}$ (E$_{m,2}$) is only ≈100 mV lower for reduction of Q (E$_{m,1}$) [110,112,161]. In solvents like DMSO with a high dielectric constant but no protons, E$_{m,2}$ is ≈500 mV lower than E$_{m,1}$, so it is much harder to reduce Q$^{\bullet-}$ than Q [162]. This extra stabilization of Q^{-2} in water cannot be credited to the Born solvation energy (Eq. (3)), as water and DMSO both have high dielectric constants. Rather it is the ability of the quinone to make hydrogen bonds to water that stabilizes Q^{-2} [70–72,163].

3.1.4. Stability of the Q$_B$ semiquinone

In contrast to what is found in water at pH 7, in the protein the semiquinones Q$_A\bullet^-$ and Q$_B\bullet^-$ are metastable species. The half time for the electron transfer from Q$_A\bullet^-$ back to P$_{860}^+$ to reform the ground state is 100 ms, while the half time for P$^+$Q$_B\bullet^-$ to charge recombine to the ground state is ≈1 s (Eq. (5)) [164]. The anionic Q$_B\bullet^-$ has an E$_m$ that is ≈200 mV more positive than for ubiquinone in water, indicating the site stabilizes the semiquinone [154]. While the anionic semiquinone has lost solvation energy in the protein it is stabilized by pair-wise interactions with the protein backbone dipoles, nearby side chains and a nearby non-heme iron [61,131–133,135,136]. With a pK$_{a,sol}$ of 4.9, if the anion were destabilized in the quinone binding site by only a few kcal/mol, the first quinone reduction would be coupled to proton binding [165]. However, both the Q$_A$ and Q$_B$ binding sites prefer the anionic semiquinone [166–168].

3.1.5. The stability of Q$_B^{-2}$

The Q^{-2} state is significantly less stable in the Q$_B$ site than it is in water [154]. A simple explanation for this can be derived from the Born equation (Eq. (3)). The solvation energy for Q^{-2} is ≈four times that of Q$^{\bullet-}$ since it depends on the square of the charge of the species. The desolvation penalty for Q^{-2} is much more severe than for Q$^{\bullet-}$ when they are moved into the protein binding site, lowering the E$_m$. In contrast the interactions with charges and dipoles vary qualitatively as described by Coulomb's law so they change linearly with the charge. Thus, the favorable interactions of the protein with Q^{-2} are only twice that of Q$^{\bullet-}$. This results in Q$^{\bullet-}$ being stabilized relative to solution in the Q$_B$ site but Q^{-2} being higher in energy than it would be in solution. The difference in stability of QH$^{\bullet-}$ and Q^{-2} in water and the Q$_B$ site changes the sequence of electron and proton transfers. In the protein this yields a metastable Q$_B\bullet^-$, a transient kinetic intermediate of QH$_B^{\bullet}$, reduction of the protonated semiquinone by Q$_A\bullet^-$ to form QH$_B^-$ and rapid, downhill binding of the second proton [169]. The sequence is thus ET, PT, ET and PT (the lower path in Eq. (7a)). In solution Q^{-2} is more stable and the sequence is ET. ET, PT and PT (the upper sequence in Eq. (7a)).

3.1.6. The role of the protein environment around Q$_B$

The Q$_B$ site is surrounded by a large group of ionizable residues, enriched in acids [127,133]. This structure modifies both the quinone E$_m$ and pK$_a$ and also serves as a proton reservoir and a proton pathway to the quinone. The protein tunes Q$_B$ so its E$_m$ is ≈60 mV more positive than Q$_A$ despite being identical compounds. There has been significant computational analysis of how the protein accomplishes this tuning [61,105,134,135,154,170,171]. Interestingly, no other pair of quinones can substitute for ubiquinone at both Q$_A$ and Q$_B$, indicating the protein interacts with this specific compound in a special way that is yet unkown [172–175].

Q$_B^-$ is stabilized by rearrangement of protons in the cluster of surrounding amino acids [61,135,171]. Without the transfer of protons amongst the acids near the Q$_B$ site the reaction fails, as can be seen by the electron transfer from Q$_A$ to Q$_B$ freezing out at ≈200 K [151,176,177]. The reaction also slows with a pK$_a$ of 9.8, as a proton from the acidic cluster of Glu L212 and Asp L 210 and 213 near Q$_B$ is lost from the protein [147,164]. Without a proton in the cluster electron transfer from Q$_A\bullet^-$ to Q$_B$ is uphill and so proton binding from solution becomes rate determining. Mutational analysis identifies GluL212 as the key residue with a pK$_a$ near 9.8 [178,179].
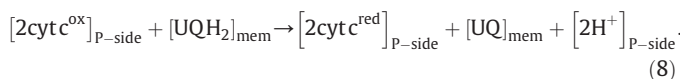
3.1.7. Thermodynamic vs kinetic stabilization of the semiquinone

The quinone system in RCs also demonstrates the balance between kinetic and thermodynamic stabilization of intermediate states in a reaction. It is important for the semiquinone in Q$_A$ or Q$_B$ sites to not be released from their binding sites. This can be accomplished by thermodynamically stabilizing the semiquinone intermediate. However, a very stable Q$_A\bullet^-$ will not be a good electron donor nor will a too stable Q$_B\bullet^-$ accept a second electron. Rather the quinones have been shown experimentally and computationally to be kinetically trapped in the binding sites [136,138]. Thus, neutral quinones bind and dissociate from the protein in milliseconds, while both the on and off rates for anionic analogs are >10,000 times slower.

---

[1] The qualitative discussion of quinones in solution will the same for the biologically active ubiquinone, plastoquinone, which is used in PSII and menaquinone, which is used in some bacterial RCs and in PSI. The specific values for E$_m$s and pK$_a$s are given for ubiquinone. A dot is used in this section to indicate the species is a semiquinone, with an unpaired electron.

3.1.8. Contribution of RCs to the proton gradient

Within the cell QH_2 is released into the intramembrane quinone pool. The quinone is reoxidized in the bc_1 complex in the Q_o site, a binding site where protons are released into the P-side of the membrane. Overall photosynthetic bacteria use cyclic electron flow involving RCs and the bc_1 complex to move protons across the membrane. P_{860}^+ oxidizes cyt c as the RCs reduce ubiquinone, pulling two protons from the N-side of the membrane onto QH_2. The bc_1 complex uses the electrons from QH_2 to rereduce two cytochromes c, but now the two protons from QH_2 are released from a binding site on the other side of the membrane (Q_O) into the P-side of the membrane [180–183]. Thus, the overall reaction in the bc_1 complex is:

$$\left[2\,cyt\,c^{ox}\right]_{P-side} + [UQH_2]_{mem} \rightarrow \left[2\,cyt\,c^{red}\right]_{P-side} + [UQ]_{mem} + \left[2H^+\right]_{P-side}. \tag{8}$$

Thus, combining Eqs. (5) and (8) shows no overall chemistry is done if the RCs and bc_1 complex are considered to be one unit, but the coupled reaction adds to the proton gradient.

3.1.9. Conclusion

RCs add to the proton gradient by vectorial redox chemistry. Contrasting the reactions of quinones in protein and in solution provides insight into how the protein tunes their proton coupled redox chemistry. Two turnovers of the protein are initiated by absorption of two photons, leading to the uptake of two protons to Q_B from the N-side of the membrane. The product QH_2 is released into the membrane. The Q_B binding site is near the N-side, needing only a relatively short path to bring protons in from the surface. There is no transmembrane proton pathway so protons cannot leak from the P-side of the membrane to protonate the quinones. The $pK_{a,sol}$ for oxidized Q is below 0 so it will be deprotonated, while the $pK_{a,sol}$ of the doubly reduced species are >10. These values are not much changed in the protein ensuring two protons will be bound to the double reduced quinone to make QH_2. However the differences in how water and proteins stabilize the protonation and redox intermediates leads to a different reaction sequence in the two environments.

3.2. Proton release from the oxygen evolving complex of PSII

PSII from green plants and bacterial RCs are both classified as type II reaction centers and so have many similarities [184]. There are differences in the cofactor choices in that PSII uses chlorophyll a and pheophytin a rather than bacteriochlorophyll a and bacteropheophytin a as core cofactors. Plastoquinone replaces ubiquinone at the Q_A and Q_B sites [185]. PSII also has a set of tightly bound antenna chlorophylls not found in RCs as well as a heme and additional carotenoids that provide alternative electron transfer pathways [186–188]. In PSII the initial electron transfer sequence may start from the excited state of a bridging chlorophyll rather than from the structural dimer as in RCs. However, the electron transfers on the reducing side are very similar in PSII and RCs. As in bacterial RCs the electron proceeds from the chlorophylls to the pheophytin to Q_A and on to Q_B, forming a doubly reduced quinone after two turnovers. Q_B reduction is expected to use the sequence ET, PT, ET and PT as is found in RCs, leading to uptake of two protons from the N-side of the membrane (Eq. (7a)) [189–192].
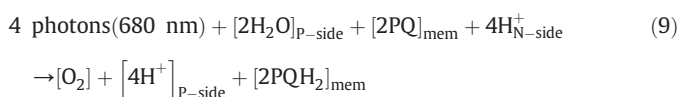
3.2.1. Contrasting how RCs and PSII add to the proton gradient

The important difference between RCs and PSII is that the primary absorption in PSII is at 680 nm, which provides 400 meV extra energy compared with the bacterial RCs, which uses 860 nm photons [8,121]. The extra energy is used to make P_{680} (E°_m 1.2 V) [193] much more

oxidizing that P_{860} (E_m 0.45 V) [194]. The difference in the oxidizing side of the reaction in PSII and RCs allows green plant photosynthesis to make more substantial contributions to the stored energy in the cell [195]. Combining the overall chemistry of the RCs (Eq. (5)) and bc_1 complex (Eq. (8)), 2 photons lead to 2 protons being transferred from the N- to P-side without any lasting chemistry being done. In contrast, the more oxidizing, P-side of PSII removes electrons from H_2O, a cheap high potential substrate. Water releases protons on the P-side adding to the proton gradient while cyt c does not. The evolutionary innovation of using water as a terminal electron donor allows green plant photosynthesis to create a linear electron transfer chain composed of PSII, the cytochrome b_6f complex and PSI [43]. Photons excite the chlorophylls in P_{680} (in PSII) and P_{700} (in PSI) to low potential. The overall process moves the electrons from water up in energy to reduce NADP ($E^{\circ}_{m,7}$ of -0.32 V) in the sequence known as the Z-scheme [196–199]. Thus, green plant, oxygenic photosynthesis can provide both a transmembrane proton gradient and reduced substrates, while bacterial, anoxygenic photosynthesis primarily only adds to the proton gradient.

3.2.2. The PSII reaction sequence

The overall reaction in PSII is (Fig. 1c):

$$4 \text{ photons}(680 \text{ nm}) + [2H_2O]_{P-side} + [2PQ]_{mem} + 4H_{N-side}^+ \tag{9}$$

$$\rightarrow [O_2] + \left[4H^+\right]_{P-side} + [2PQH_2]_{mem}$$

PQ is plastoquinone. The pK_a of the oxidized plastoquinone is below zero while it is above 10 when reduced so protons are bound from the N-side when the quinone is reduced. Thus, the redox chemistry of UQ and PQ are similar (Eq. (7a)). Likewise, reduced water has a high pK_a of 15.7, while it is very low for the oxidized O_2, which has a very small proton affinity. Thus, the input of four photons leads to the oxidation of two waters to O_2, with the release of 4 protons to the P-side of the membrane.

3.2.3. The oxygen evolving complex (OEC)

The electron transfer sequence from P_{680} to PQ_B is similar to the transfer from P860 to UQ_B found in RCs (Q-1) [192]. The oxidizing side of the reaction sequence constitutes the main difference between RCs and PSII. Water is oxidized by the oxygen evolving complex (OEC), a $Mn_4O_5Ca^{+2}$ cluster built with four Mn and a Ca^{+2} ion bridged by five oxygens (Fig. 4) [200,201]. While redox active quinones, chlorophylls and tyrosines are found in a variety of proteins the OEC is unique to PSII [202,203]. It appears that biology learned to remove electrons from water, the ubiquitous solvent, once and this invention was retained [204–206].

Four electrons must be removed from two waters to generate O_2. The OEC is oxidized 4 times through 4 turnovers of P_{680} generating four S states [26,207–209]. S_1, which is the stable state in the dark, has a Mn oxidation state of Mn(III,III,IV,IV) [210]. Following loss of electrons in the S_2 and S_3 states the unstable S_4 state has accumulated 4 holes at sufficiently high potential to oxidize water. Two waters are oxidized in a single step to O_2 without any release of damaging, partially oxidized oxygen intermediates to form the reduced S_0 state Mn(III,III,III,IV), which will be oxidized back to S_1. The reaction sequence that leads to refilling the hole on P_{680}^+ is:

$$OEC(S_i)Y_ZHP_{680}^{\bullet+} \rightarrow OEC(S_i)Y_Z^{\bullet}P_{680} + H^+ \rightarrow OEC(S_{i+1})Y_ZHP_{680}. \tag{10}$$

Here Y_ZH is a Tyr in the reduced, protonated ground state. $Y^{\bullet}_Z$ is the species that has been oxidized and deprotonated. $OEC(S_i)$ is the oxygen evolving complex in the ith S state. $P_{680}^{\bullet+}$ is the oxidized and P_{680} is the ground state of the primary chlorophyll donor in PSII. Here a dot on Y or P_{680} indicates an unpaired electron.
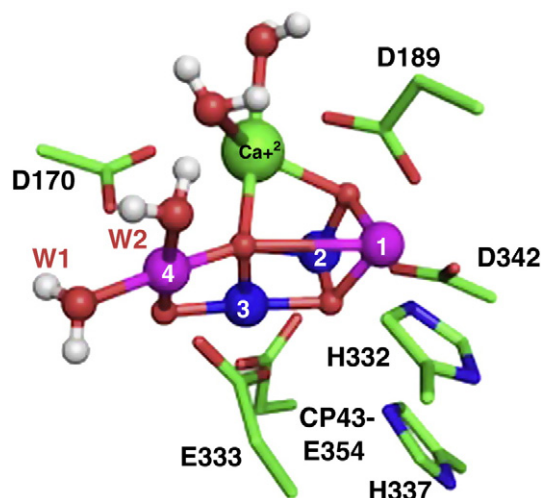
Fig. 4. The $Mn_4O_5Ca^{+2}$ cluster of the OEC in the S_1 state and the amino acids and waters that are the first coordination shell ligands of the Mn. Coordinates from DFT simulations [261]. Blue spheres: Mn(IV); Magenta spheres: Mn(III). The Mn cluster is coordinated in the protein by D170, D342, E333, E189, H332 and the terminal A344 from the D1 subunit and E354 from the CP43 subunit of the PSII [24]. In addition, to the core complex there are two waters attached to the dangler Mn (Mn(4) and two waters to the Ca^{+2}.

3.2.4. The redox active Tyr

P_{680}^+ is first reduced by Y_Z, a redox active tyrosine, which then extracts an electron from the OEC [26,190,211–213]. The $pK_{a,sol}$ of an isolated Tyrosine is 10.9 [214], while the $pK_{a,sol}$ of the oxidized $Y \cdot H^+$ is -2 [215], so a proton must be lost as the Tyr is oxidized. However, Y_Z is only transiently deprotonated, as it must rebind a proton to oxidize the OEC [216]. The neutral His190, which is in hydrogen bonding distance to Y_Z is the hydrogen bond acceptor from the ground state Tyr [202]. Following Y_Z oxidation a reassignment of proton ownership likely leads to $HisH^+$ becoming a H bond donor to the deprotonated, oxidized $Y\bullet$. This proton rocking mechanism can keep the proton close so when Y_ZH is oxidized by $P_{680}\bullet^+$ and $Y\bullet$ is reduced by the OEC, long distance proton transfers are not needed [202,203]. It is interesting that tyrosine, which has a very large pK_a shift between ground and oxidized state requiring coupled proton and electron transfer is chosen to be the intermediate on the electron transfer pathway rather than a non-protonable cofactor such as a heme. The $E_{m,sol}$ for Tyrosine oxidation is at least 600 mV [212] and may be >900 meV [217]. It is likely chosen since a group with a very positive potential is needed to be able to oxidize the OEC in each S state.

3.2.5. Complexes designed as models of the OEC

One open question is why Mn is used in the OEC. The first row transition metals, Mn, Fe, Co, Ni, Cu and Zn, are used as the basis of the active site clusters in different proteins [218]. It is not always well understood why a particular metal is chosen to catalyze different chemistry in proteins [219–226]. Most types of reactions use specific metals. However, flexibility can be seen. For example, different superoxide dismutases (SOD) use the $Mn^{+3/+2}$, $Fe^{+3/+2}$, $Ni^{+3/+2}$ and $Cu^{+2/+1}$ redox couples to form the core of their active sites [227–229]. Even for oxygen chemistry different cofactors are chosen. While the OEC uses a high valent Mn_4O_5Ca complex to oxidize water to O_2 [230–233], the Binuclear Complex (BNC) of cytochrome c oxidase (CcO) uses a heme and a Cu to reduce O_2 back to water (Section 3.4). PSII and RCs have a non-heme iron in a structural capacity between the quinones and can use iron within bound hemes that function in secondary electron transfer pathways.

The key criteria for how well a given metal will work in a given site involves a number of factors [218,220–223,225,226,234–236] including

the intrinsic electron affinity of the metal and the preferred type, number and orientation of the first shell ligands in each redox state. For the first row transition metals the d orbital configuration is responsible for most of the electrochemical properties of the metal and the degree to which it can be modified by the ligands. For example, the octahedral aqua $[Mn(H_2O)_6]^{+3/+2}$ oxidation potential is 1.5 V while it is 0.77 for the $Fe^{+3/+2}$ redox couple [237]. Because Fe^{+2} has one more d orbital electron than Mn^{+2}, the repulsion between the electrons lowers the oxidation potential. The behavior of the metal will then be tuned by the ligands. For example, anionic or electron donating ligands will lower the E_m of a cluster and raise the pK_a of associated protonatable sites.

3.2.6. pK_as of hexaaquo-metal complexes

An important factor that helps determine if a particular metal–ligand cluster can carry out proton coupled electron transfer is the pK_a of the titratable ligands (Fig. 2) [50,238,239]. The simplest metal complexes with protonatable ligands have six waters bound in an octahedral arrangement [237]. These are models for the systems of interest here as the oxo-manganese OEC binds terminal waters that are deprotonated and oxidized to O_2. As will be seen below CuB in CcO binds a product oxygen atom that will change from hydroxyl to water as the Cu is reduced (Section 3.4).

As found for the quinone reduction and water oxidation, tight coupling between redox and protonation chemistry requires that the pK_a in the oxidized state be below the ambient pH while it shifts to be above it when the cluster is reduced. The initial deprotonation of many transition metal aqua complexes behave in this manner (Tables 1a and 1b). Large shifts in pK_a of 7–10 pH units are seen on reduction of the metal. Each of these complexes has a pK_a for deprotonation to $M^{+3}(H_2O)_5(OH^-)$ between 0.7 and 2.9, while in the M^{+2} state the pK_a ranges from 7.5 to 10.7. In the oxidized state they will have at least one water deprotonated at pH 7, while with the exception of Cu all 6 waters will be fully protonated in the reduced state. Thus, these simple complexes will all participate in robust proton coupled redox reactions in water at neutral pH. In these hexaaquo complexes there are 6 pK_as, one for each water. The pK_a of each succeeding water is higher because of the interactions amongst the hydroxyls in the cluster [237].

3.2.7. pK_as of oxo-manganese complexes

The dependence of $pK_{a,sol}$ on Mn oxidation has been investigated in a number of compounds such as a Mn-bpy complex (**1**) (complex numbers refer labels in to Table 1b) and several Mn-salpn complexes (**2** to **7**) that were designed as models for the $Mn_4O_5Ca^{+2}$ cluster that is the core of the OEC (Table 1b) [240–242]. These are di-μ-oxo bridged complexes.

Table 1a
The pK_as of mononuclear metal complexes determined in water.

	$n = 2$	$n = 3$	$n = 4$	ΔpK_a	Ref
$[Mn(H_2O)_6]^{+n}$	10.7	0.7		10	[103]
$[Fe(H_2O)_6]^{+n}$	10.1	2.2		7.9	[103]
$[Co(H_2O)_6]^{+n}$	9.6	2.9		6.7	[103]
$[Zn(H_2O)_6]^{+n}$	8.96	–		–	[103]
$[Cu(H_2O)_6]^{+n}$	7.53	–		–	[103]
Aquo-His-c- heme	10.9	9.6		1.3	[108,112]
Fe-complex 1		6.6	5.7	0.9	[115]
Fe-complex 2		4.4	2.3	1.1	[114]
Mn-complex 1		5.8	4.1	1.7	[115]
Mn-complex 2		4.4	1.8	2.6	[114]

n represents the oxidation state of the metal. Complex I [5,10,15,20-tetrakis (2,6-dimethyl-3-sulfonatophenyl) porphyrinato]; complex 2 [5,10,15,20-tetrakis (2,6-dichloro-3-sulfonatophenyl) porphyrinato]; the Aquo-His-c- heme is a microperoxidase with the heme attached to an octapeptide with one axial His ligand and two peripheral Cys ligands.

Table 1b
The measured pK_a of the µ-oxo and terminal waters in di-Mn complexes.

	Complex no.	Solvent	Mn(III,III)	Mn(III,IV)	Mn(IV,IV)	ΔpK III$_2$ → III,IV	ΔpK III,IV → IV$_2$	Ref
The pK_a of the µ-oxo-bridges								
Bpy	1	Water	11	2.3	–	8.7		[117]
H-salpn	2	ACN	–	24.5	13.4		11.1	[122]
3,5-Di(Cl)-salpn	3	ACN	–	20.0	10.8		9.2	[122]
3,5-Di(NO$_2$)-salpn	4	ACN	–	13.3	5.0		8.3	[122]
5-(OCH$_3$)-salpn	5	ACN	–	–	14.1			[123]
5-(Cl)-salpn	6	ACN	–	–	11.5			[123]
5-(NO$_2$)-salpn	7	ACN	–	–	6.8			[123]
The pK_a of the terminal waters								
Terpy	8	Water	–	4<	1.8			[124]
L(3,5-Cl)	9	Mix	–	10	<0			[119]
L(3,5-H)	10	Mix	19	11	<0	8		[119]
L(3,5-*t*-Bu)	11	Mix	20	10	<0	10		[119]

(bpy = 2,2′-bipyridyl), (salpn = N,N′-bis(salicylidene)-1,3-propanediamine), (terpy = 2,2′:6′,2″-terpyridine), (L = 2-hydroxy-1,3-bis(3,5-X-salicylideneamino)propane), (X = Cl, H, di-2*tert*-butyl), and Mix = 16 M water/ACN.

The bridging oxygens can be in the µ-oxo^{-2} or µ-hydroxy^{-1} state. The di-Mn-terpy complex (**8**) and Mn$_2$L$_2$ (**9** to **11**) complexes add terminal waters, which are an important feature of the OEC. The Mn-salpn complexes have anionic ligands with a net charge of −2 on each Mn, modeling the Asp and Glu ligands that bind the OEC to PSII. In all of these complexes the ligand $pK_{a,sol}$ shifts on Mn oxidation by 8 to 11 pH unit when the di-Mn core is oxidized from Mn(III,IV) to Mn(IV,IV) (Mn salpn complexes) or from Mn(III,III) to Mn(III,IV) (Mn-bpy complex) [241,243]. The terminal water ligand to a Mn experiences a $pK_{a,sol}$ shift of ~9 pH units on reduction of the Mn$_2$L$_2$ complex [244], similar to that found for the hexaaqua Mn complex.

The $pK_{a,sol}$ of the oxo-manganese complexes in Table 1b in the same redox state differ by over 20 pH units. One reason is the difference in the solvent that was used for the measurements. The $pK_{a,sol}$ for the hexaaqua complexes (Table 1a) as well as the measurements for the bridging oxygens in the bpy complex and terminal water in the terpy complex were determined in water (Table 1b). The salpn complexes were measured in acetonitrile and dichloromethane. There are rather regular shifts when experiments allow comparison of the $pK_{a,sol}$ for the same complexes in acetonitrile and water. Shifts of 7.5 ± 1 pH units [245] to 6.7 ± 0.9 pK_a units have been found. The latter value was derived from recent computational studies of the bpy and salpn complexes [246]. If a $pK_{a,sol}$ shifts by 7 pH units because of the solvent, the $pK_{a,sol}$ of the Mn(III,IV) H-salpn structures are still ≈13 pH units higher than that found for the bpy complex in the same redox state. This difference in proton affinity shows the influence of replacing the neutral bpy ligands with negatively charged salpn ligands. The pK_as in the modified salpn complexes show how the presence of electron donating NO$_2$ or withdrawing Cl, modifies the pK_a of the bridging oxygens. However, the substantial pK_a shift of 8-11 pH units on oxidation is remarkably independent of the effect of the solvent, the addition of electron donating or withdrawing groups or the starting redox state in all of these oxo-manganese complexes.

3.2.8. pK_a shifts accompanying oxidation of the OEC

The overall OEC reaction oxidizes two waters leading to the release of four protons. As the OEC is oxidized through the four S states, protons are lost along with electrons to keep a large positive charge from building up on the cluster [213,232,247]. These protons may be released from the bridging oxygens in the cluster core, from the terminal waters or liganding amino acids or from amino acids surrounding the cluster (Fig. 4). Oxidation of the Mn lowers the pK_as of both bridging oxygens and terminal waters by at least 8 pH units in model complexes designed to study the chemistry of the OEC (Table 1b). However, this large pK_a

shift does not ensure proton loss. The metal oxidation will be coupled to proton loss only if the pK_as of the ligands shift from a value higher than the physiological pH when reduced to one lower than the pH when oxidized (Fig. 2). The OEC can be viewed as a set of three oxomanganeses dimers for comparison with the model complexes (Table 1b) [248]. The S$_1$ state would be made up of one Mn(III,III) dimer and 2 Mn(III,IV) dimers. The oxygen bridging a Mn(III,III) dimer should have a pK_a higher than the physiological pH in complexes with either neutral, bpy or anionic, salpn ligands. The oxidation of one Mn(III) center in the next catalytic step to form a Mn(III,IV) unit will shift the pK_a of the µ-oxo by 9 pH units, which is likely to initiate proton loss. In the more advanced catalytic intermediates the proton release is expected to be from the terminal waters.

3.2.9. Theoretical analysis of the OEC

Theoretical models based on density functional theory (DFT) simulations have been used to explore potential mechanisms for how the OEC oxidizes water. There are a variety of DFT studies of the protonation states of the bridging and terminal oxygens in different S states [249–260]. For example, the Batista group has studied S$_1$ [261], Neese has studied S$_2$ [262] and Siegbahn S$_2$, S$_3$ and S$_4$ [263]. The S$_1$ model [261] has Mn(2) and Mn(3) in the (IV) oxidation state, while Mn(1) and the dangler Mn (Mn(4)) are in the (III) oxidation state (see Fig. 4 for position of the four Mn in the OCE). This S$_1$ model has all the µ-oxo bridges deprotonated and all terminal waters protonated. Comparing this structure with the S$_2$ model [262] predicts that the dangler Mn is oxidized forming S$_2$ and one of the waters attached to this Mn loses a proton to become a hydroxyl. This assignment for the Mn oxidation agrees with recent HYSCORE experiments [264]. Consistent with the S$_1$ structure, all of the bridging oxygens are deprotonated. However, isotope-edited infrared spectroscopy shows that the S$_1$ to S$_2$ transition in intact PSII does not involve proton release [265]. If a proton is released from the OEC it would need to be bound by amino acids in the protein. A model with proton release from the OEC on each oxidation step is supported by the comparison of the catalytic cycle with fewer protein subunits, which has a proton release pattern (1,1,1,1) rather than (1,0,1,2) in the intact PSII [266].

3.2.10. Proton transfer pathways

The protons released from the OEC must find their way to the surface 35 Å away. Recent work shows a potential role for essential Cl ions in this transfer. A Cl is found in the structure near D2–K317 and D1–D61, which is on a putative proton channel leading from the OEC

[24]. MD and Monte Carlo simulations show that this Asp–Lys pair can form a stable salt-bridge in the absence of the Cl. Cl thus appears to be essential to allow protons to exit from the OEC [267].

3.2.11. Conclusion

PSII adds to the proton gradient by vectorial redox chemistry. Protons are released to the P-side of the membrane when water is oxidized to O_2. In addition, as in RCs, quinone reduction on the N-side leads to proton uptake and release of QH_2 into the membrane. The $pK_{a,sol}$ of O_2 and plastoquinone shift by more than 10 pH units when they are reduced, so redox chemistry is tightly coupled to proton binding and release. Model compounds have been used to gain insight into the chemistry of the OEC, a Mn_4O_5Ca cluster that is the catalyst for water oxidation in PSII. The OEC will be oxidized four times in the S state cycle so it can to oxidize water in a single step without generating partially oxidized, reactive oxygen species. Protons are released from the OEC and/or the protein during the S state cycle, keeping the cluster from becoming so positive that it cannot advance to higher oxidation states. If the OEC behaves like oxomanganese model complexes, the pK_as of the bridging oxygens and terminal waters should shift substantially as each Mn is oxidized leading to strong coupling between the loss of electrons and protons.

3.3. The bacteriorhodopsin proton pump

Bacteriorhodopsin is the simplest and best studied classical proton pump [27,31,76,268,269]. Absorption of a photon initiates a reaction cycle that removes a proton from the cell interior (N-side) and releases one to the outside (P-side) adding to the proton gradient. The overall reaction is simply (Fig. 1a):

$$photon(568\ nm) + H^+_{N-side} \rightarrow H^+_{P-side}. \tag{11}$$

3.3.1. Requirements for a proton pump

While bacteriorhodopsin is like PSII and RCs in that light provides the energy to increase the proton gradient, the reaction mechanism is fundamentally different. The photosynthetic systems use redox reactions occurring on opposite sides of the membrane with no proton transfer through the protein (Sections 3.1 and 3.2). Stable products such as reduced quinone, oxidized cytochrome and O_2 are formed by the reactions (Eqs. (5) and (9)). In contrast, in bacteriorhodopsin a proton pathway traverses the protein. The path consists of acidic and basic amino acids, which will change ionization states in metastable intermediates, linked by waters and polar groups that can transiently hold or release a proton. A successful pump must take a proton from the N-side and release it to the P-side, even though it is thermodynamically favorable for them to move in the opposite direction (Fig. 3). Therefore an efficient pump must have a gate that controls the access of the protein interior to the outside. The gate ensures that when a proton is bound the access to the N-side is open, while in the step where a proton is released there is only an open path to the P-side. In other steps protons are retained within the protein and transferred internally. The driving force for individual proton transfer steps is modulated by changes in the proton affinity of key residues or of cluster of residues caused by small structural rearrangements. The affinity changes are described by shifts in residue pK_as (Eq. (3)).

3.3.2. Key residues in bacteriorhodopsin

Studies of bacteriorhodopsin have revealed a great deal about how this protein structure supports proton pumping. It is a 7-helix bundle with a retinal group covalently attached to the protein via a Schiff base (SB) at Lys 216 [30,270,271]. The reaction sequence is triggered by the retinal cofactor absorbing light causing it to change from the all-*trans* to the 13-*cis*, 15-*anti* configuration. The other key players in the pump are protein side chains found in three well,

separated locations (Fig. 5). The central cluster (CC) consists of the SB, D85 and D212. The exit cluster (EC) is made up of E194 and E204 near the P-side side of the protein. D96 is a relatively isolated residue near the N-side. Metastable intermediates showing changes in protonation states in bacteriorhodopsin have been characterized by FTIR and Raman measurements [27,272–277]. A number of intermediates have been trapped by mutation and freezing, generating a remarkable series of X-ray crystal structures [278,279]. The structures show small conformational changes that modulate the pK_as of key residues in the CC and EC to drive proton transfers [27].

3.3.3. The bacteriorhodopsin reaction cycle

The description of the reaction cycle focuses on the intermediates that show changes in protonation state. The early, short lived states (denoted K and L) will not be discussed. In the ground state all three residues of the CC are ionized and one proton bound (Table 2). Retinal isomerization then moves the SB towards the N-side
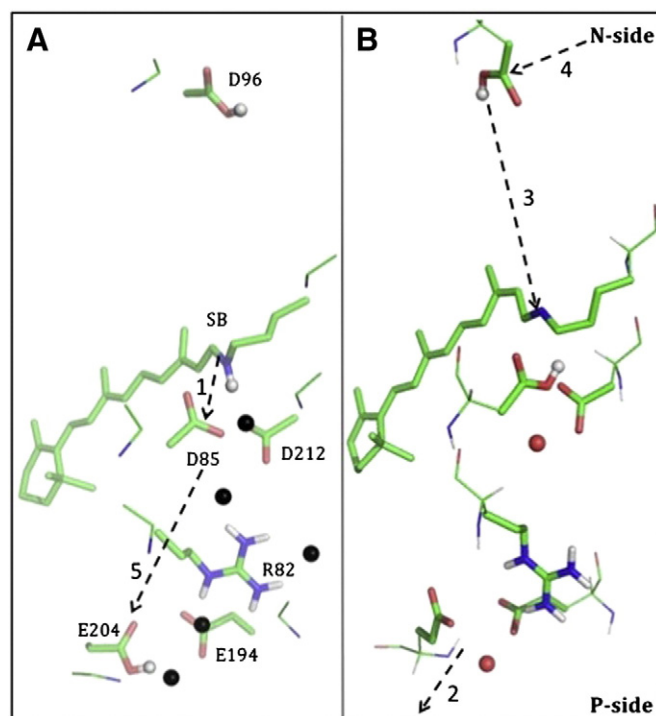

Fig. 5. Proton transfers in bacteriorhodopsin. (A) The structure with the *trans*-retinal found in the ground and O states. The protonation pattern shown with the central cluster (CC): ((SBH⁺)(D85⁻)(D212⁻)), exit cluster (EC): ((E204H)(E194⁻) and D96 protonated represents the ground state (the protons to be transferred are shown as white spheres). Proton transfer 1 occurs in the initial stages after retinol isomerization and 5 occurs in the O state with a *trans* retinal. (B) The structure with the *cis*-retinal found in the M1 and M2, and N and N′ states. The protonation pattern shown with ((SB)(D85H)(D212⁻)), ((E204⁻)(E194⁻) and D96 protonated would be found in the N′ state. The key changes in the structure that modify the equilibrated proton distribution are the rotation of the Schiff Base away from the acids in the CC, the separation of E194 and E204 in the EC moving E204 out of plane here and the rotation of R82 away from the CC towards the EC. Proton transfers 2, 3 and 4 happen in the protein with a *cis*-retinal. The proton transfer sequence is shown by the labeled arrows. (1) The early M state is formed by proton transfer within the CC, from the retinal-Schiff base (SB) to D85 4 Å away. (2) The late M state is formed by the EC cluster releasing a proton to the N-side of the membrane. (3) The N state is formed by proton transfer from D96 to the SB ≈ 12 Å away. (4) D96⁻ is rapidly reprotonated from the N-side to form the N′ state. In the states prior to N the CC has one proton. In the N and N′ states the CC binds two protons. The N′ to O transition involves retinal isomerization back to the all-*trans* state without any proton transfers. (5) The transition from the O to the ground state transfers the second proton in the CC to the EC ≈ 15 Å away.

further from the two acids, raising the pK$_a$ of D85 relative to the SB (Fig. 5). The proton transfers from the SB to D85, generating the early M state (M1). In the ground and M states the net charge on the CC is −1, with only a proton shift within the CC yielding the M1 state. When ionizable groups interact strongly it can be better to view the proton affinity of the cluster than the individual residues. Thus, the CC with the SB, D212 and D85 has 8 possible protonation states (2^3, where each of the 3 residues can be in one of 2 protonation states) ranging in charge from +1 to −2. Each transition between cluster protonation states can be described by a pK$_a$. The pK$_a$ for the CC to bind a second proton to have a net charge of zero is higher in the M1 state, but remains below 7 so no additional protons are bound [59]. Changes in exit cluster (EC) protonation yield the M1 to M2 transition. From the BR until M1 state the EC binds one proton with a cluster pK$_a$ of ≈10. In M2 the EC pK$_a$ shifts to ≈5 releasing a proton to the nearby P-side of the membrane [27]. Two small conformational changes modify the thermodynamic landscape for EC protonation (Fig. 5). The most critical is that in the protonated state the two EC acids are within hydrogen bonding distance keeping a proton bound in the cluster. The shift in the structure allows the acids to move apart and the proton to be released. Additional stabilization of the doubly deprotonated EC is added by R82, which has moved 1.6 Å away from the CC towards the EC on retinal isomerization [270].

The net proton affinity of the CC changes in the M states to move the cluster pK$_a$ above 7 so it now binds another proton. The doubly protonated CC is stabilized by the changes in position of the residues within the CC and by motion of the positively charged R82 away from D85 towards the EC [268]. Although the CC and EC are separated by ≈8 Å, in the membrane embedded protein the electrostatic interactions are quite long-range. Thus, proton release from the EC in M2 stabilizes proton binding to the CC in the N state. The key to proton pumping is that the proton comes from D96 rather than from the P-side via the EC. D96 has a pK$_a$ > 11 in the ground state [280]. D96$^−$ is unstable and is rapidly reprotonated from the P-side forming the N′ state. In the N′ state the SB returns to the *trans* configuration without any proton shifts, moving the SB nitrogen to the N-side close to D85. D85, which is protonated in the N and O states now releases its proton to the EC, returning the protein to the ground state.

The intermediate protonation states described here are shown to be in a metastable equilibrium in the isomerized, *trans* structure [31,60,270,278,281]. They can be seen by optical measurements and are found to last for microseconds to milliseconds. They can be trapped by freezing or by single mutations that slow the next steps in the proton transfer in a crystal. Simulations that evaluate the Boltzmann distribution of protonation states generally show the low energy protonation states do shift appropriately between different

trapped structures. Other proton distributions required in the reaction pathway are unstable intermediates. This includes states with the deprotonated D96$^−$ (N state) [280] and a system where the charge on the central cluster is −1 and the exit cluster has a −2 charge (M2).

3.3.4. The role of hydronium

Protonated water species are generally considered to play an important role in proton transport reactions [282]. Within bacteriorhodopsin FTIR measurements show the EC proton is shared between at least one water and the two acids in the ground state, indicating a hydronium with unusual stability [277,283]. However, the hydronium may not be a critical part of the mechanism. Changing either EC Glu to Asp localizes the proton on either E204 (in the E194D mutant) or D204 (in the E204D mutant). Thus, when mutation destabilizes the hydronium the system continues to pump protons utilizing the EC acids as the proton storage site [283].

3.3.5. Proton pathways and the gating mechanism

The structures of bacteriorhodopsin trapped in different intermediates have provided the information to show how small changes can modify the thermodynamic landscape leading to a series of metastable intermediates in different protonation states [59,284]. The remaining questions concern the gating mechanism to control the direction of proton transfer. The proton must be released from the EC into the low pH, P-side, and rebound via D96 from the high pH, N-side of the membrane. The proton transfer path can be divided into 4 steps: from the P-side to the CC via D96 (in the late M to N transition); the internal transfer from the SB to D85 (to form M1 after retinal isomerization); the internal transfer from D85 to the EC (O to ground state); and the release to the P-side from the EC M1 to M2 The temporal sequence of proton transfers from the N-side to the P-side is thus not a series of physically sequential transfers (Fig. 5, Table 2). Rather, there is a short internal transfer within the CC, then proton output to the P side followed by input from the N side to restore a state with a total of 2 protons bound to the CC and EC. Lastly proton transfer from the CC to EC resets the system in the ground state.

Proton transfer pathways must contain waters or polar groups that can be transiently protonated. Comparison of the different structures provides some qualitative suggestions for how each segment of the pathway can facilitate or slow transfer in different stages of the reaction cycle. On isomerization of the retinal, a proton is transferred from the SB to the nearby D85, which is 4 Å away to form the M1 state. Nearby residues T89 and D212 and a crystallographic water are in a position to mediate the proton transfer [285]. With the *cis* retinal moving the SB nitrogen away from D85, the pathway within the CC may break, blocking the transfer back from D85 to the SB, forcing the

Table 2
The intermediates in BR reaction cycle.

State	Ionization state of key groups	Retinal	D96	SB	D85	EC	Access	State formed by
bR	D96H:SBH$^+$D85$^−$D212$^−$:ECH	*Trans*	H	H		H		Ground state
M1	D96H:SB D85H D212$^−$:ECH	*Cis*	H	→	H	H	Inside	H transfer within CC
M2	D96H:SB D85H D212$^−$:EC$^−$	*Cis*	H		H	H$_P$→	P-side	H release from EC
N	D96:SBH$^+$D85H D212$^−$:EC$^−$	*Cis*	→	H	H		Inside	H transfer D96 → SB
N′	D96H:SBH$^+$D85H D212$^−$:EC$^−$	*Cis*	→H$_N$	H	H		N-side	H binding to D96
O	D96H:SBH$^+$D85HD212$^−$:EC$^−$	*Trans*	H	H	H			Retinol isomerization
BR	D96H:SBH$^+$D85$^−$D212$^−$:ECH	*Trans*	H	H	→	H	Inside	H transfer CC → EC

The intermediates in the bacteriorhodopsin photocycle discussed here start with M1, the state formed after the first proton transfer from the SB to D85 [27,31]. EC: The extracellular cluster is composed of E194 and E204 and is found near the P-side of the protein. In the table EC$^−$ indicates both E194 and E204 are deprotonated; ECH indicates that the exit cluster has a proton on one of the glutamic acids or on a nearby water. SB, D85 and D212 make up the central cluster (CC). D96 is on the N-side of the protein. →H$_N$: proton bound from the N-side of the membrane and H$_P$→: proton released to the P-side of the membrane. Other arrows indicate the direction of the internal proton transfers that lead to the changes in intermediates. For example the arrow in the SB column in the M1 state indicates the proton that is first found on D85 in the M1 state comes from the SB.

proton to come to the SB from the N-side via D96 rather from the P-side via the EC and D85.

Upon protonation of D85 in the M1 state, a proton is released from the EC, 8 Å away to the P-side extracellular surface [277,284,286]. The EC does not get protonated until the O to bR transition when the SB has returned to its *trans* conformation. The EC must be protonated by internal proton transfer from the protonated D85 rather than by binding from solution on the P-side. The crystal structures suggest that the connection between the EC and CC may be stronger in the states with the *trans* retinal such as the bR and O states. In crystal structures of the bR ground state, a three-dimensional network of hydrogen-bonded side chains and waters is seen [270]. One continuous chain can be formed through 2 waters that connect D85 to R82, and another 2 waters that connect R82 to E194. In the M2 state crystal structures, E194 has a better connection to R82, in its downward position. However, the loss of crystallographic water and the downward shift of R82 breaks the connection between D85 and R82 [287]. This change in connectivity could help to close the proton transfer pathway between the CC and the EC in the M and N states.

In the M2 to N′ transition a proton is transferred from the cytoplasm to the SB via D96. In the ground state there is no pathway for proton transfer between D96 and the CC. After the retinal is isomerized, the Schiff base nitrogen is displaced toward the N-side of the protein, facilitating its protonation from D96. By the M intermediates there are changes in the C, F, and G helices on the N-side of the protein, allowing formation of a water chain for the proton conduction from the N-side via D96 to the SB [277,281,288].

3.3.6. Conclusion

The crystal structures of bacteriorhodopsin trapped in metastable, protonated states combined with extensive spectroscopic and computational studies shows how a proton pump can transfer protons across a protein. The sequence of proton transfers is driven by small structural changes triggered by retinal isomerization leading to a shift in the backbone of helix by $\approx$0.5–0.7 Å [30,270,271]. The CC and EC put protonatable residues very close together so they have strong electrostatic interactions. These interactions change significantly with small changes in structure. Pulling the SB away from the two acids in the CC stabilizes proton transfer from the SBH$^+$ to D85$^-$. Separating the E204 from E194$^-$ in the EC releases the proton on E204 or a hydronium to form the M2 state. The interaction between the EC and CC stabilize a state where the two clusters hold two protons. One proton is always in the CC. The second is in the EC in the ground state with a *trans* retinal or in the CC in the N′ state with the *cis* retinal [59,289]. The shift of the proton in the N′ state is stabilized by the cationic R82 moving from the CC, which now has two protons bound, to the EC, which has lost a proton. In bacteriorhodopsin the key to pumping is that the proton does not transfer a proton from the EC to the CC in the M1 to M2 state transition with the *cis* retinal but releases it from the EC to the low pH side of the membrane. It is only in the O state, which has a *trans* retinal while retaining the N′ state protonation pattern, that the pathway between the CC and EC is used to return the proton from D85 to the EC cluster.

3.4. Vectorial proton transfers and proton pumping in cytochrome c oxidase (CcO)

When plants began to carry out oxygenic photosynthesis, life on earth changed. Now atmospheric oxygen could be used as the terminal electron acceptor in aerobic respiration, producing significantly more energy than the anaerobic metabolic chains. Cytochrome c oxidase (CcO) is the protein that reverses the OEC reaction in many organisms, reducing oxygen to water using electrons from cytochrome c [7,32–41,45,290–292]. CcO combines the functions of a true
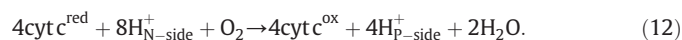
transmembrane proton pump such as bacteriorhodopsin (Section 3.3) and systems, such as RCs and PSII (Sections 3.1 and 3.2), where the proton gradient is increased by vectorial redox reactions occurring on different sides of the protein. The result is that CcO moves 8 charges across the membrane coupled to the reduction of O_2, which requires 4 electrons.

RCs, PSII and bacteriorhodopsin all use a photon to initiate the reaction cycle. This makes it possible to synchronize the reaction for study, and can provide remarkable insights into the metastable reaction intermediates. In special cases it has been possible to trap and crystallize structures in different metastable protonation [278,279] or redox [293–296] states. CcO is a more conventional protein where the reaction is started by diffusion of the reactants. It is therefore harder to monitor the individual intermediates through the whole reaction cycle, thus there are still more consequential questions that remain unanswered.

Combining information about the reaction intermediates with the structures of RCs, PSII and bacteriorhodopsin, reveals motifs that lead to proton transfers. These basic mechanisms are: (1) The use of redox reactants such as quinones and O_2 where the pK$_a$ of reduced species is above the pH, while the pK$_a$ is below the pH when it is oxidized (Section 3.1–3.2, Fig. 2). The active sites are arranged with respect to the membrane so that reduction occurs on the N-side of the membrane and oxidation on the P-side. (2) The use of amino acids nearby the redox sites that will bind and release protons in response to the charge change on a redox cofactor. The acids surrounding the quinone binding sites provide an example. (3) The use of clusters of amino acids whose group pK$_a$ can be shifted significantly by small changes in structure as found in bacteriorhodopsin (Section 3.3, Fig. 5). CcO reactions will be described here to consider how the reaction cycle leads to binding of the chemical protons needed for O_2 reduction from the N-side as well as the translocation of pumped protons from N- to P-side of the protein.

3.4.1. The CcO reaction sequence

The overall CcO reaction is (Fig. 1d):

$$4\text{cyt c}^{\text{red}} + 8\text{H}^+_{\text{N-side}} + O_2 \rightarrow 4\text{cyt c}^{\text{ox}} + 4\text{H}^+_{\text{P-side}} + 2\text{H}_2\text{O}. \qquad (12)$$

The desired product is not water, but rather the transfer of protons that add to the transmembrane gradient. The reaction takes place in the Binuclear Center (BNC) which consists of Heme a3, an a-type heme with one His ligand and one position that is free to bind oxygen, hydroxyl or water; CuB, a Cu with 3 His ligands and a position to bind a hydroxyl or water, and Y288,[2] which is a redox active tyrosine [297]. On average each of the four electron transfers to the BNC needed to reduce one O_2 results in two charges transferred across the membrane. One electron from cyt c is imported from the P-side to meet a proton coming from the N-side in the BNC, which is deeply buried in the protein. CcO differs from the RCs and PSII that use vectorial redox chemistry to add to the proton gradient (Fig. 2) in that the protons travel a long pathway from the N-side to the redox cofactors in CcO. Thus, a proton is taken up from the N-side and delivered to the BNC as part of the oxygen reduction chemistry. In addition, each time CcO is reduced a second proton is taken up on the N-side and pumped to the P-side.

In CcO four electrons are accumulated in the BNC before O_2 binds [7,291]. This pre-reduction of the active site allows the O=O bond to be broken without forming any high-energy oxygen redox

---

[2] The amino acid numbering for the *Rps. sphaeroides* CcO will be used here. The key residues are Y288 and E286. These are numbered as Y280 and E278 in Bovine CcO and Y244 and E242 in *Paracoccus denitrificans* CcO.
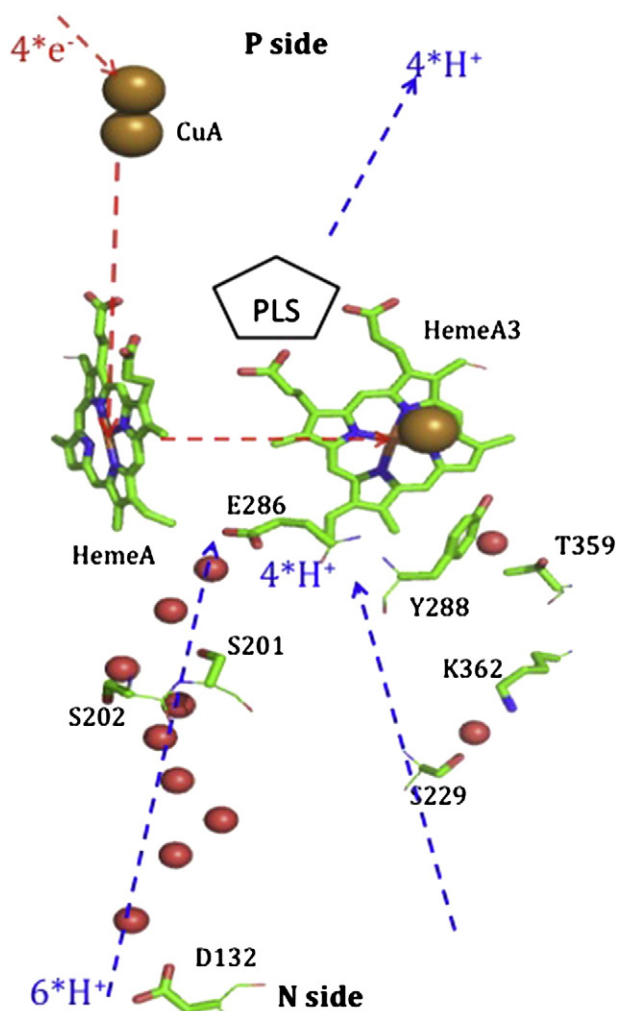
Fig. 6. The key groups in cytochrome c oxidase (CcO). The gray pentagon represents the Proton Loading Site (PLS) that transiently holds the proton that is being pumped. Electron transfers are shown by red arrows, proton transfers by blue arrows. The overall reaction sequence: the protein is reduced by cytochrome c on the P-side of the membrane. Electrons are passed from CuA to Heme A to the Binuclear Center (BNC) consisting of Heme A3, CuB and Y288. *Rb. sphaeroides* residue numbers are used here. Each time CcO is reduced two protons are bound from the N-side of the membrane. One proton is taken up either via the D (Left) or K (right) channel and passed to the BNC via E286 or K362. These protons are used for the chemistry that produces H₂O. In addition, 4 pumped protons are taken up through the D channel. These are passed to the P-side of the membrane via the PLS, which is located on the P-side of the protein near the BNC.

intermediates. This strategy is similar to that used in PSII where 4 holes are accumulated before water oxidation commences [42,298–300]. In each CcO reduction step cyt c reduces CuA, a two copper cluster, which in turn reduces Heme a (Fig. 6). Heme a then passes electrons to the BNC. CcO is primed in the R state $(Fe^{+2}CuB^{+1}YOH)$ to bind and reduce O₂. Four electrons are donated to O₂, two from Heme a3, one from CuB and one from Y288 to generate the BNC in its most oxidized form with $Fe^{+4}=O^{-2}$, $CuB^{+2}OH^-$ and YO•, denoted the P$_M$ state. Addition of 4 electrons to rereduce the BNC leads the protein through a sequence of metastable states designated F, O, E and R.

There is good evidence that protons are pumped across the membrane each time the protein is reduced, not only in the step where electrons are transferred to O₂ [301–303]. The formally exothermic reaction that breaks the O=O bond occurs in the R to P$_M$

transition. Somehow each of the next 4 reductions of the BNC by cyt c produces enough energy to pump two charges across the membrane against an electrochemical potential of ≈220 mV [304]. Estimates are that in the mitochondria each electron transfer from cytochrome c to the BNC could liberate 500 meV [7]. As two charges are transferred across the membrane this would give an efficiency of over 80%. The current assumption is that the sequence of proton transfers in the pumping mechanism is the same for each stage of BNC reduction and so it is insensitive to which group is being reduced or protonated in the BNC [37,305,306]. However, each of the 4 reductions of the BNC has a different driving force since, while the electron donor is always Heme a, the acceptor is CuB^{+2}, ferryl or ferric Heme a3, or radical Y288 (YO•). In addition, the driving force for proton binding will change in each step as the pK$_a$ shift on cofactor reduction is different for each group. These pK$_a$ shifts will be discussed here.

3.4.2. The pK$_a$ shifts coupled to reduction of the groups in the binuclear center (BNC)

As found in RCs and PSII, one mechanism to bind protons is to have the redox reaction induce large pK$_a$ shifts within the cofactor and its first coordination shell ligands. The OEC is an oxo-manganese complex, where each oxidation shifts the pK$_a$ of the bridging oxygens or terminal waters by 8-10 pH units (Section 3.2, Table 1b). Its four bridging oxygens and two terminal waters thus provide a reliable source for protons to be lost into the P-side of the membrane as the system moves through the four oxidation states in the S-state cycle. A similar mechanism is seen in the reducing side of RCs (Section 3.1) and PSII, which takes place on the N-side of the protein where the oxidized quinone reactant has a pK$_a$ < 0 while it is > 10 in the doubly reduced product.

In CcO the chemical protons are bound into the BNC from the N-side as the various constituents are reduced by electron transfer from cyt c^{red}, through Heme a into the BNC. In the P$_M$ state, formed after O₂ reduction, the BNC redox and protonation state is: $Fe^{+4}=O^{-2}$, $Cu^{+2}OH^-$ and YO•. The oxygens on the ferryl Heme a3 and CuB are the products of bond breaking chemistry. The proton on the CuB-hydroxyl is likely donated by Y288 along with an electron [297,307]. The R state, formed after 4 reductions of the BNC is: $Fe^{+2}-H_2O$, $CuB^{+1}-H_2O$, and YOH, indicating 2 protons have been bound by the ligand to heme a3, one to the ligand to CuB and one to Y288. The waters on Heme a3 and CuB must be released before the next O₂ is bound in the R state. The increase in pK$_a$ as each element is reduced will provide a measure of the driving force for proton binding.

The first question is what is the intrinsic chemistry in solution of the three groups that make up the BNC. The protein, especially within the confines of the BNC, can modify these values but the choice of these groups in the active site sets the initial parameters for proton uptake (Eqs. (2a) and (2b)). Thus, if the pK$_a$ is not above the pH in the reduced state and below it in the oxidized state there will be no chemical protons involved with that reduction step (Fig. 2) [49]. The question is what is the shift in the pK$_a$ going from the $Fe^{+4}=O^{-2}$ to aquo-Fe^{+3} to aquo-Fe^{+2} Heme a3, from oxidized to reduced aquo-CuB and from oxidized, deprotonated YO• to the ground state, YOH.

3.4.3. The pK$_a$ of oxygen species on hemes

Hemes are a common and well studied redox cofactors found in many proteins. Within proteins the heme electrochemistry is modified to span > 800 mV [66,308]. For example, in strains of bacterial RCs with an attached cytochrome subunit such as *Bl. viridis* the heme E$_m$s range over 450 mV [309]. With a titratable axial ligand such as water, hemes are able to participate in redox coupled proton transfers. Heme a3 binds an axial oxygen ligand derived from the

substrate O_2 that will be protonated to form the product water as the reaction progresses.

To understand the basic chemistry of aquo-hemes, the $pK_{a,sol}$ for hemes in water have been measured in microperoxidases, which are c-type hemes retaining a short peptide with two peripheral Cys ligands and one axial His ligand. A second axial ligand can be water or a tighter binding added solute such as imidazole [310–316]. The pK_as in the aquo-heme complexes behave quite differently than the hexa-aquo-metal complexes (Table 1a). The water/hydroxyl $pK_{a,sol}$ for both reduced, Fe^{+2}, and oxidized, Fe^{+3}, states are above 7. Thus, in solution the heme water ligand will already be protonated in the oxidized, ferric state and so will not bind a proton when the heme is reduced. In addition, the change in $pK_{a,sol}$ for the bound water is only 1.3 pH units so the protonation reaction is almost independent of the heme redox state. A small $pK_{a,sol}$ shift on reduction is a feature of porphyrin based complexes. Adding an electron withdrawing chloride or donating methyl group on the ring or changing the central metal to Mn will shift the $pK_{a,sol}$. However, all of the porphyrin based complexes shift the pK_a of an axial water ligand on metal oxidation by only 0.9 to 2.6 pH [317,318]. Changes in the other axial ligand to the metal will also change the $pK_{a,sol}$ without greatly influencing the pK_a shift on oxidation. For example the aqua-His-c-type heme pK_a is higher than found in the Fe based form of complex 2, which has two axial water ligands (Table 1a). The His ligand is more electron donating than is the water, raising the proton affinity of the titrating water.

Thus, if the aquo-Heme a in CcO behaves like it would in solution, the pK_a of $Fe^{+4}{=}O^{-2}$ is likely to be <4 [319,320] while the $pK_{a,sol}$ for protonation of $Fe^{+3}OH^-$ is >9 so oxidation of the ferryl Heme a3 should be coupled to binding of 2 protons (Tables 1a and 1b). The next step of heme reduction only increases the $pK_{a,sol}$ for proton binding to $Fe^{+2}OH^-$ to 10.9 [311,314]. This weak coupling between the reduction of ferrous Heme a3 and proton binding poses a challenge for our understanding a mechanism where each reduction of the BNC should be coupled to a large pK_a shift to provide the energy needed to pull protons out of the N-side of the membrane.

3.4.4. Redox active amino acids

Tyr is used as a redox active cofactor in both PSII and CcO as well as in other proteins. The chemistry of redox active amino acids such as Tyr and Trp are well characterized [211,214,321,322]. For Tyr the $pK_{a,sol}$ of the ground state is 10.9 [323]. When it is oxidized the $pK_{a,sol}$ shifts to be <0 [215]. Thus, Tyr is a species that will need to lose a proton when an electron is lost [217]. In solution, Y288 is a Tyr covalently attached to His284, one of the ligands to CuB [307]. The His–Tyr bond moves the Tyr $pK_{a,sol}$ from 10.8 for the unmodified residue to 8.9 stabilizing the YO^- state and reducing the strong coupling between electron and proton binding when $YO\bullet$ is reduced [324]. However, the pK_a shift between an oxidized and reduced Y288 should be sufficient so that reduction of $YO\bullet$ should be coupled to proton uptake.

CuB is bound to three His and one oxygen derived from the O_2. If it behaves like an aquo Cu species described in Table 1a, than CuB^{+2} is likely to bind a hydroxyl while CuB^{+1} should have a pK_a as much as 9 pH units higher and so would bind a water. Thus, CuB is expected to show proton binding coupled to reduction.

The pK_a shifts that bind chemical protons will be different for each step in the reduction of CcO. A mechanism where the same number of protons are taken into the BNC despite changes in the underlying chemistry of the individual groups can also be seen in a comparison of the P_M and P_R states. The P_R state is formed when Heme a is reduced at the time of O_2 reduction so that Heme a, not Y288, becomes the donor of the 4th electron. The proton needed

for the CuB hydroxyl is still donated by Y288. The P_R state of the BNC is: $Fe^{+4}{=}O^{-2}$, $Cu^{+2}OH^-$ and YO^- [37]. The pumping stoichiometry is the same no matter if the protein goes through the P_M or the P_R states [38,325–327], despite the stability of the deprotonated YO^- with a $pK_{a,sol}$ of 8.9 being much smaller than that of the oxidized $YO\bullet$ with a $pK_{a,sol} < 0$.

3.4.5. CcO proton pathways

CcO has two well studied proton uptake channels (Fig. 6) [328–332]. If the cycle starts in the oxidized CcO (O state), with Fe^{+3}, CuB^{+2} and YOH, the K channel takes up 2 protons coupled to the first two electrons added to the protein. These protons are used for chemistry [5]. The D channel is the pathway for the other 6 protons, two that will be used for chemistry and the other 4 that will be pumped. D132 is at the beginning of the D channel and E286 at the end. The K channel is named for the required K362 inside the protein near the BNC. In each proton pathway there are a few polar residues and in the D channel, a fairly continuous chain of waters [333,334]. Thus, the proton intake paths are narrow, well-defined, water filled channels. The proton outlet is a more complex region towards the P-side, above the BNC and Heme a. For example, on the P side of *Rps. sphaeroides* CcO there are ≈ 18 acidic and basic residues and 4 propionic acids within the 10 Å centered around the D-propionic acid of Heme a3, providing competing pathways for proton release [335]. The pumped proton is assumed to be transiently bound within this region at a Proton Loading Site (PLS) on the P-side of the BNC and then released to that side of the membrane [305,306,336–338]. The complexity of the outlet channel makes it difficult to see how protons are blocked from entering from the P-side when they are needed for O_2 reduction chemistry.

3.4.6. The shifting thermodynamic landscape for proton transfers in CcO

In the other proteins described in this review the reaction sequence goes through proton transfer intermediates that are sufficiently stable to be seen and characterized. This indicates the conformation or redox changes shift the thermodynamic landscape sufficiently that the metastable pK_as for the groups in question have moved from being below physiological pH in one state to above it in another. It has been more difficult to get experimental information about the sequence of changes that occur in CcO, as it lacks the inherent advantages of proteins such as bacteriorhodopsin, RCs and PSII where the reaction is initiated by light and so can be synchronized and intermediates followed through a natural reaction cycle. Computer simulations have provided some possible explanations for how the equilibrium pK_as are modified in possible CcO intermediates [36,49,291,338–349].

There are several methods that have been designed to initiate a portion of the CcO reaction cycle with a flash of light. In one method photoactive ruthenium complexes are attached to oxidized cyt c. The light activated Ru complex reduces the cyt c, which in turn initiates the electron transfer to CuA [350]. Another method uses CcO in the R state with CO bound in the BNC [351]. A flash of light dissociates the CO and allows O_2 to bind and move from the R to P_M to F states if CuA and Heme a are oxidized or from R to P_R to F states if they are reduced [37]. Spectroscopic measurements show that protons are transferred to the BNC prior to the electron transfer from Heme a to the BNC. It is assumed that the chemical proton enters the BNC after the pumped proton is passed to the PLS [326]. The approximate position of the PLS within the protein is becoming better defined, but there is still uncertainty about which group or groups contribute [305,306,336].

The choreography posited for the CcO reaction cycle requires that, synchronized with each reduction of the BNC by Heme a, a proton is taken from the N-side. This is transferred via the K channel into the BNC (in the O to E and E to R transitions) or from

the D channel (in the P to F and F to O transitions). In addition, a proton is transported through the D channel to the PLS and then released into the P-side of the membrane. Current mechanisms thus assume a number of intermediates that the protein passes through four times during a full O_2 reduction cycle. K362, which appears to have an abnormally low $pK_a < 7$ [49,328], would need to be protonated transiently during proton transfer to the BNC. E286, with a $pK_a \approx 10$ in the P_R to F transition state [37,352,353], is deprotonated transiently as it serves as the conduit for proton transfer via the D channel. In the P and O states some mechanism is needed to determine if the proton on E286 will be released to the BNC or pushed on to the PLS [347,354–359]. A residue or cluster of residues serving as the PLS on the P-side of the protein needs to bind and release a proton coupled to electron and proton transfers to the BNC. A sequence with these transitions must be incorporated into the reaction for all steps of the BNC reduction cycle [291,349,360,361]. The question that remains is how the free energy of these intermediate states and the kinetics of transfer between them are controlled within the CcO structure.

3.4.7. Structural information about conformational changes in CcO

There are now several structures of reduced and oxidized bovine [40,362] and *Rb. sphaeroides* [41,334] CcO. The CcO structures show only modest changes. For example, the dominant change in the *Rb. sphaeroides* structures are in the K channel, appearing to keep it open in the oxidized protein, and cause it to be closed by a hydrogen bond in the reduced protein. This structural change may determine if the K or D channel is used for the chemical protons, but does not affect the structure near E286, the BNC or the PLS as would be needed to shift their proton affinities through the pumping cycle.

The lack of clear conformational changes in the crystal structures that would affect the proton affinity of key sites may be a result of CcO undergoing the same pumping steps in each BNC redox state. Thus, the oxidized and reduced crystal structures may be stopped at the same, lowest energy protonation states. Likewise simulations that simply interrogate the equilibrium protonation states in CcO in different BNC redox states show surprisingly little protonation changes coupled to BNC chemistry [49]. Thus, the lack of changes in structures and simulations support a model where the proton transfer intermediates are not controlled by the redox state of the BNC.

3.4.8. Modulating group pK_as in the proton loading site (PLS)

The pumping model assumes that a proton, released from E286 will be transiently bound within the group of residues on the P-side of the BNC denoted the PLS. The best candidates are the propionic acids attached to Heme a or a3 or His 334, a ligand to CuB [348,363–365]. If the His binds a proton in the R state where CuB is reduced and releases it in the P_M state where it is oxidized then CcO would be using the pK_a shift of a first coordination shell ligand to couple electron and proton transfer. However, since a proton is pumped in each stage of BNC reduction, the His would need to bind and release a proton in steps that do not change the CuB redox state. The shift in the pK_a of the His to below physiological pH would thus need to be controlled by long-range electrostatics rather than by strong coupling of electron and proton affinity in a metal complex [363].

The propionic acids, are attached to the heme by single bounds so are affected by the heme redox state by long-range electrostatics. The oxygens on the propionic acids are ≈ 8 Å from the center of the heme as they are in most hemes [366]. The separation between the CC and EC in bacteriorhodopsin is 8 Å and these groups retain sufficient interaction to mutually perturb each others pK_a by ≈ 2 pH units (Section 3.3) [59]. In addition, both the His 334 and the propionic acids exist in a cluster of ionizable residues so they are susceptible to small conformational changes

leading to significant changes in protonation such as found in bacteriorhodopsin.

3.4.9. Changing the pK_as of E286, the likely proximal proton donor to the BNC and the PLS

E286 and K362 on the D and K proton pathways have shifted pK_as so they are neutral in their low energy states [49]. Neither E286 or K362 are surrounded by other ionizable groups as would be needed for a mechanism where small change in conformation would change their pK_as sufficiently to change the equilibrium ionization state as found in the CC and EC clusters in bacteriorhodopsin. Thus, without a surrounding cluster that helps to stabilize the binding and release of protons these residues are more likely to behave like D96 in bacteriorhodopsin being deprotonated only transiently in a short-lived state.

3.4.10. Conclusion

The BNC active site of CcO is deeply buried in the protein, but it carries out redox chemistry using only protons from the N-side of the membrane. The reaction cycle is driven by the O_2 reduction reaction, which is sufficiently endergonic to support additional proton transfers via a proton pumping mechanism. There remain many open questions about CcO. Each of the four electron and proton transfers into the active site is to a different cofactor and so has a different driving force. Cofactors such as aquo-heme are used in the BNC that have very small shifts in $pK_{a,sol}$ when they undergo redox chemistry. Yet all steps of BNC reduction appear to be coupled to proton pumping and to the uptake of protons used for chemistry from the N-side. In addition, as CcO has added a pump to a system with vectorial redox chemistry a mechanism is now needed to keep protons for O_2 reduction from coming from the P-side of the protein, while the pumped protons must exit to this side. The mechanism to control access is unknown. The key residues in the pump are not found in clusters of ionizable residues as found in bacteriorhodopsin so are less likely to use small conformational changes to modify their proton affinity. Thus, the investigation of these four well-studied proteins shows that analysis of the structures can provide insight into the underlying mechanisms but does not solve all problems.

Acknowledgements

References

[1] P.R. Rich, The molecular machinery of Keilin's respiratory chain, Biochem. Soc. Trans. 31 (2003) 1095–1105.
[2] P.R. Rich, A perspective on Peter Mitchell and the chemiosmotic theory, J. Bioenerg. Biomembr. 40 (2008) 407–410.
[3] D.G. Nicholls, Mitochondrial ion circuits, Essays Biochem. 47 (2010) 25–35.
[4] M. Jastroch, A.S. Divakaruni, S. Mookerjee, J.R. Treberg, M.D. Brand, Mitochondrial proton and electron leaks, Essays Biochem. 47 (2010) 53–67.
[5] D.D. Newmeyer, S. Ferguson-Miller, Mitochondria: releasing power for life and unleashing the machineries of death, Cell 112 (2003) 481–490.
[6] J.P. Hosler, S. Ferguson-Miller, D.A. Mills, Energy transduction: proton transfer through the respiratory complexes, Annu. Rev. Biochem. 75 (2006) 165–187.
[7] P. Brzezinski, R. Gennis, Cytochrome c oxidase: exciting progress and remaining mysteries, J. Bioenerg. Biomembr. 40 (2008) 521–531.
[8] P. Heathcote, Reaction centers: the structure and evolution of biological solar power, Trends Biochem. Sci. 27 (2002) 79–86.
[9] P. Mitchell, Coupling of phosphorylation to electron and hydrogen transfer by a chemi-osmotic type of mechanism, Nature 191 (1961) 144–148.
[10] G. Oster, H. Wang, Rotary protein motors, Trends Cell Biol. 13 (2003) 114–121.

[11] R.H. Fillingame, C.M. Angevine, O.Y. Dmitriev, Mechanics of coupling proton movements to c-ring rotation in ATP synthase, FEBS Lett. 555 (2003) 29–34.

[12] D. Okuno, R. Iino, H. Noji, Rotation and structure of FoF1-ATP synthase, J. Biochem. 149 (2011) 655–664.

[13] T. Minamino, K. Imada, K. Namba, Molecular motors of the bacterial flagella, Curr. Opin. Struct. Biol. 18 (2008) 693–701.

[14] Y. Sowa, R.M. Berry, Bacterial flagellar motor, Q. Rev. Biophys. 41 (2008) 103–132.

[15] J. Orlowski, S. Grinstein, Diversity of the mammalian sodium/proton exchanger SLC9 gene family, Pflugers Arch. 447 (2004) 549–565.

[16] E. Padan, L. Kozachkov, K. Herz, A. Rimon, NhaA crystal structure: functional–structural insights, J. Exp. Biol. 212 (2009) 1593–1603.

[17] A. Accardi, A. Picollo, CLC channels and transporters: proteins with borderline personalities, Biochim. Biophys. Acta 1798 (2010) 1457–1464.

[18] G. Feher, J.P. Allen, M.Y. Okamura, D.C. Rees, Primary processes in bacterial photosynthesis: structure and function of bacterial photosynthetic reaction centres, Nature 339 (1989) 111–116.

[19] M.R. Gunner, The reaction center protein from purple bacteria: structure and function, Curr. Top. Bioenerg. 16 (1991) 319–367.

[20] M.L. Paddock, G. Feher, M.Y. Okamura, Proton transfer pathways and mechanism in bacterial reaction centers, FEBS Lett. 555 (2003) 45–50.

[21] R.E. Blankenship, M.T. Madigan, C.E. Bauer, Anoxygenic Photosynthetic Bacteria, Kluwer Academic Publishers, 1995.

[22] J. Barber, Photosystem II: a multisubunit membrane protein that oxidises water, Curr. Opin. Struct. Biol. 12 (2002) 523–530.

[23] J. Barber, Photosystem II: the engine of life, Q. Rev. Biophys. 36 (2003) 71–89.

[24] Y. Umena, K. Kawakami, J.-R. Shen, N. Kamiya, Crystal structure of oxygen-evolving photosystem II at 1.9 A resolution, Nature 473 (2011) 55–60.

[25] T. Cardona, A. Sedoud, N. Cox, A.W. Rutherford, Charge separation in photosystem II: a comparative and evolutionary overview, Biochim. Biophys. Acta 1817 (2012) 26–43.

[26] H. Dau, I. Zaharieva, M. Haumann, Recent developments in research on water oxidation by photosystem II, Curr. Opin. Chem. Biol. 16 (2012) 3–10.

[27] S.P. Balashov, Protonation reactions and their coupling in bacteriorhodopsin, Biochim. Biophys. Acta 1460 (2000) 75–94.

[28] H. Luecke, Atomic resolution structures of bacteriorhodopsin photocycle intermediates: the role of descrete water molecules in the function of this light-driven ion pump, Biochim. Biophys. Acta 1460 (2000) 133–156.

[29] A. Onufriev, A. Smondyrev, D. Bashford, Proton affinity changes driving unidirectional proton transport in the bacteriorhodopsin photocycle, J. Mol. Biol. 332 (2003) 1183–1193.

[30] B.W. Edmonds, H. Luecke, Atomic resolution structures and the mechanism of ion pumping in bacteriorhodopsin, Front. Biosci. 9 (2004) 1556–1566.

[31] J.K. Lanyi, Proton transfers in the bacteriorhodopsin photocycle, Biochim. Biophys. Acta 1757 (2006) 1012–1018.

[32] M.K. Wikstrom, Proton pump coupled to cytochrome c oxidase in mitochondria, Nature 266 (1977) 271–273.

[33] P.R. Rich, Towards an understanding of the chemistry of oxygen reduction and proton translocation in the iron–copper respiratory oxidases, Aust. J. Plant Physiol. 22 (1995) 479–486.

[34] S. Ferguson-Miller, G.T. Babcock, Heme/copper terminal oxidases, Chem. Rev. 96 (1996) 2889–2907.

[35] V.R. Kaila, G. Hummer, Energetics of direct and water-mediated proton-coupled electron transfer, J. Am. Chem. Soc. 133 (2011) 19040–19043.

[36] Y.C. Kim, M. Wikstrom, G. Hummer, Kinetic gating of the proton pump in cytochrome c oxidase, Proc. Natl. Acad. Sci. U. S. A. 106 (2009) 13707–13712.

[37] G. Branden, R.B. Gennis, P. Brzezinski, Transmembrane proton translocation by cytochrome c oxidase, Biochim. Biophys. Acta 1757 (2006) 1052–1063.

[38] M. Wikström, M.I. Verkhovsky, Mechanism and energetics of proton translocation by the respiratory heme-copper oxidases, Biochim. Biophys. Acta 1767 (2007) 1200–1214.

[39] A.A. Konstantinov, Cytochrome c oxidase: intermediates of the catalytic cycle and their energy-coupled interconversion, FEBS Lett. 586 (2012) 630–639.

[40] S. Yoshikawa, K. Muramoto, K. Shinzawa-Itoh, M. Mochizuki, Structural studies on bovine heart cytochrome c oxidase, Biochim. Biophys. Acta 1817 (2012) 579–589.

[41] S. Ferguson-Miller, C. Hiser, J. Liu, Gating and regulation of the cytochrome c oxidase proton pump, Biochim. Biophys. Acta 1817 (2012) 489–494.

[42] G.T. Babcock, M. Wikström, Oxygen activation and the conservation of energy in cell respirations, Nature 356 (1992) 301–308.

[43] W.A. Cramer, D.B. Knaff, Energy Transduction in Biological Membranes: A Textbook of Bioenergetics, Springer-Verlag, New York, 1991.

[44] P. Mitchell, The protonmotive Q cycle: a general formulation, FEBS Lett. 59 (1975) 137–139.

[45] P. Mitchell, Chemiosmotic coupling in oxidative and photosynthetic phosphorylation. 1966, Biochim. Biophys. Acta 1807 (2011) 1507–1538.

[46] P. Mitchell, Possible molecular mechanisms of the protonmotive function of cytochrome systems, J. Theor. Biol. 62 (1976) 327–367.

[47] B.G. Malmstroem, Vectorial chemistry in bioenergetics: cytochrome c oxidase as a redox linked proton pump, Acc. Chem. Res. 26 (1993) 332–338.

[48] C.C. Moser, T.A. Farid, S.E. Chobot, P.L. Dutton, Electron tunneling chains of mitochondria, Biochim. Biophys. Acta 1757 (2006) 1096–1109.

[49] Y. Song, E. Michonova-Alexova, M.R. Gunner, Calculated proton uptake on anaerobic reduction of cytochrome c oxidase: is the reaction electroneutral? Biochemistry 45 (2006) 7959–7975.

[50] H.B. Gray, J.R. Winkler, Electron flow through metalloproteins, Biochim. Biophys. Acta 1797 (2010) 1563–1572.

[51] M.Y. Okamura, R.A. Isaacson, G. Feher, The primary acceptor in bacterial photosynthesis: obligatory role of ubiquinone in photoactive reaction centers of *Rhodopseudomonas sphaeroides*, Proc. Natl. Acad. Sci. U. S. A. 72 (1975) 3492–3496.

[52] M.R. Gunner, D.E. Robertson, P.L. Dutton, Kinetic studies on the reaction center protein from *Rhodopseudomonas sphaeroides*: the temperature and free energy dependence of electron transfer between various quinones in the Q_A site and the oxidized bacteriochlorophyll dimer, J. Phys. Chem. 90 (1986) 3783–3795.

[53] Q. Xu, M.R. Gunner, Temperature dependence of the free energy, enthalpy and entropy of $P^+Q_A^-$ charge recombination in photosynthetic reaction centers, J. Phys. Chem. B 104 (2000) 8035–8043.

[54] L.M. Utschig, Y. Ohigashi, M.C. Thurnauer, D.M. Tiede, A new metal binding site in photosynthetic bacterial reaction centers that modulates Q_A to Q_B electron transfer, Biochemistry 37 (1998) 8278–8281.

[55] M.L. Paddock, M.S. Graige, G. Feher, M.Y. Okamura, Identification of the proton pathway in bacterial reactions centers: inhibition of proton transfer by binding of Zn^{2+} or Cd^{2+}, Proc. Natl. Acad. Sci. U. S. A. 96 (1999) 6183–6188.

[56] J.M. Swanson, C.M. Maupin, H. Chen, M.K. Petersen, J. Xu, Y. Wu, G.A. Voth, Proton solvation and transport in aqueous and biomolecular systems: insights from computer simulations, J. Phys. Chem. B 111 (2007) 4300–4314.

[57] H.J. Lee, E. Svahn, J.M. Swanson, H. Lepp, G.A. Voth, P. Brzezinski, R.B. Gennis, Intricate role of water in proton transport through cytochrome c oxidase, J. Am. Chem. Soc. 132 (2010) 16225–16239.

[58] A.Y. Mulkidjanian, Conformationally controlled pK-switching in membrane proteins: one more mechanism specific to enzyme catalysis? FEBS Lett. 463 (1999) 199–204.

[59] Y. Song, J. Mao, M.R. Gunner, Calculation of proton transfers in bacteriorhodopsin bR and M intermediates, Biochemistry 42 (2003) 9875–9888.

[60] T. Hirai, S. Subramaniam, J.K. Lanyi, Structural snapshots of conformational changes in a seven-helix membrane protein: lessons from bacteriorhodopsin, Curr. Opin. Struct. Biol. 19 (2009) 433–439.

[61] E. Alexov, M.R. Gunner, Calculated protein and proton motions coupled to electron transfer: electron transfer from Q_A^- to Q_B in bacterial photosynthetic reaction centers, Biochemistry 38 (1999) 8254–8270.

[62] D.A. Cherepanov, A.Y. Mulkidjanian, W. Junge, Transient accumulation of elastic energy in proton translocating ATP synthase, FEBS Lett. 449 (1999) 1–6.

[63] C. Fufezan, J. Zhang, M.R. Gunner, Ligand preference and orientation in b- and c-type heme-binding proteins, Proteins 73 (2008) 690–704.

[64] J. Mao, K. Hauser, M.R. Gunner, How cytochromes with different folds control heme redox potentials, Biochemistry 42 (2003) 9829–9840.

[65] K. Hauser, J. Mao, M.R. Gunner, pH dependence of heme electrochemistry in cytochromes investigated by multiconformation continuum electrostatic calculations, Biopolymers 74 (2004) 51–54.

[66] Z. Zheng, M.R. Gunner, Analysis of the electrochemistry of hemes with E_ms spanning 800 mV, Proteins 75 (2009) 719–734.

[67] A.P. Gamiz-Hernandez, G. Kieseritzky, A.S. Galstyan, O. Demir-Kavuk, E.W. Knapp, Understanding properties of cofactors in proteins: redox potentials of synthetic cytochromes b, Chemphyschem 11 (2010) 1196–1206.

[68] J.J. Warren, J.M. Mayer, Proton-coupled electron transfer reactions at a heme-propionate in an iron-protoporphyrin-IX model compound, J. Am. Chem. Soc. 133 (2011) 8544–8551.

[69] H. Shalev, D.H. Evans, Solvation of anion radicals: gas-phase versus solution, J. Am. Chem. Soc. 111 (1989) 2667–2674.

[70] J.E. Heffner, C.T. Wigal, O.A. Moe, Solvent dependence of the one-electron reduction of substituted benzo-and napthoquinones, Electroanalysis 9 (1997) 629–632.

[71] J.E. Heffner, J.C. Raber, O.A. Moe Jr., C.T. Wigal, Using cyclic voltammetry and molecular modeling to determine substituent effects in the one-electron reduction of benzoquinones, J. Chem. Educ. 75 (1998) 365.

[72] K. Sasaki, T. Kashimura, M. Ohura, Y. Ohsaki, N. Ohta, Solvent effect in the electrochemical reduction of p-quinones in several aprotic solvents, J. Electrochem. Soc. 137 (1990) 2437–2443.

[73] M.R. Gunner, E. Alexov, A pragmatic approach to structure based calculation of coupled proton and electron transfer in proteins, Biochim. Biophys. Acta 1458 (2000) 63–87.

[74] D. Bashford, Macroscopic electrostatic models for protonation states in proteins, Front. Biosci. 9 (2004) 1082–1099.

[75] E.B. Garcia-Moreno, C.A. Fitch, Structural interpretation of pH and salt-dependent processes in proteins with computational methods, Methods Enzymol. 380 (2004) 20–51.

[76] M.R. Gunner, J. Mao, Y. Song, J. Kim, Factors influencing energetics of electron and proton transfers in proteins. What can be learned from calculations, Biochim. Biophys. Acta 1757 (2006) 942–968.

[77] A. Warshel, A. Dryga, Simulating electrostatic energies in proteins: perspectives and some recent studies of pKas, redox, and other crucial functional properties, Proteins 79 (2011) 3469–3484.

[78] E. Alexov, E.L. Mehler, N. Baker, A.M. Baptista, Y. Huang, F. Milletti, J.E. Nielsen, D. Farrell, T. Carstensen, M.H. Olsson, J.K. Shen, J. Warwicker, S. Williams, J.M. Word, Progress in the prediction of pKa values in proteins, Proteins 79 (2011) 3260–3275.

[79] J.E. Nielsen, M.R. Gunner, B.E. Garcia-Moreno, The pKa cooperative: a collaborative effort to advance structure-based calculations of pKa values and electrostatic effects in proteins, Proteins 79 (2011) 3249–3259.

[80] L.I. Krishtalik, The medium reorganization energy for the charge transfer reactions in proteins, Biochim. Biophys. Acta 1807 (2011) 1444–1456.

[81] A.J. Cohen, P. Mori-Sanchez, W. Yang, Challenges for density functional theory, Chem. Rev. 112 (2012) 289–320.

[82] P.E. Siegbahn, M.R. Blomberg, Quantum chemical studies of proton-coupled electron transfer in metalloenzymes, Chem. Rev. 110 (2010) 7040–7061.

[83] P. Geerlings, F. De Proft, W. Langenaeker, Conceptual density functional theory, Chem. Rev. 103 (2003) 1793–1873.

[84] G. Roos, P. Geerlings, J. Messens, Enzymatic catalysis: the emerging role of conceptual density functional theory, J. Phys. Chem. B 113 (2009) 13465–13475.

[85] M. Orio, D.A. Pantazis, F. Neese, Density functional theory, Photosynth. Res. 102 (2009) 443–453.

[86] R.B. Murphy, D.M. Philipp, R.A. Friesner, A mixed quantum mechanics/molecular mechanics (QM/MM) method for large-scale modeling of chemistry in protein environments, J. Comput. Chem. 21 (2000) 1442–1457.

[87] S.C. Kamerlin, M. Haranczyk, A. Warshel, Progress in ab initio QM/MM free-energy simulations of electrostatic energies in proteins: accelerated QM/MM studies of pKa, redox reactions and solvation free energies, J. Phys. Chem. B 113 (2009) 1253–1272.

[88] S.P. de Visser, Density functional theory (DFT) and combined quantum mechanical/molecular mechanics (QM/MM) studies on the oxygen activation step in nitric oxide synthase enzymes, Biochem. Soc. Trans. 37 (2009) 373–377.

[89] H.M. Senn, W. Thiel, QM/MM studies of enzymes, Curr. Opin. Chem. Biol. 11 (2007) 182–187.

[90] R.A. Friesner, Ab initio quantum chemistry: methodology and applications, Proc. Natl. Acad. Sci. U. S. A. 102 (2005) 6648–6653.

[91] R.E. Georgescu, E.G. Alexov, M.R. Gunner, Combining conformational flexibility and continuum electrostatics for calculating pKas in proteins, Biophys. J. 83 (2002) 1731–1748.

[92] G. Kieseritzky, E.-W. Knapp, Optimizing pKa computation in proteins with pH adapted conformations, Proteins 71 (2008) 1335–1348.

[93] Y. Song, J. Mao, M.R. Gunner, MCCE2: improving protein pKa calculations with extensive side chain rotamer sampling, J. Comput. Chem. 30 (2009) 2231–2247.

[94] L.I. Krishtalik, Continuum electrostatics of proteins: experimental test with model solvents and the method of the proteins pK calculations, J. Chem. Phys. 319 (2005) 316–329.

[95] E.G. Alexov, M.R. Gunner, Incorporating protein conformational flexibility into the calculation of pH-dependent protein properties, Biophys. J. 72 (1997) 2075–2093.

[96] D. Bashford, M. Karplus, The pKas of ionizable groups in proteins: atomic detail from a continuum electrostatic model, Biochemistry 29 (1990) 10219–10225.

[97] P. Beroza, D.R. Fredkin, M.Y. Okamura, G. Feher, Protonation of interacting residues in a protein by a Monte Carlo method: application to Lysozyme and the photosynthetic reaction center of *Rhodobacter sphaeroides*, Proc. Natl. Acad. Sci. U. S. A. 88 (1991) 5804–5808.

[98] A.-S. Yang, M.R. Gunner, R. Sampogna, K. Sharp, B. Honig, On the calculation of pKas in proteins, Proteins Struct. Funct. Genet. 15 (1993) 252–265.

[99] J. Khandogin, C.L. Brooks III, Toward the accurate first-principles prediction of ionization equilibria in proteins, Biochemistry 45 (2006) 9363–9373.

[100] A. Aleksandrov, S. Polydorides, G. Archontis, T. Simonson, Predicting the acid/base behavior of proteins: a constant-pH Monte Carlo approach with generalized born solvent, J. Phys. Chem. B 114 (2010) 10634–10648.

[101] S.G. Itoh, A. Damjanovic, B.R. Brooks, pH replica-exchange method based on discrete protonation states, Proteins 79 (2011) 3420–3436.

[102] M. Machuqueiro, A.M. Baptista, Is the prediction of pKa values by constant-pH molecular dynamics being hindered by inherited problems? Proteins 79 (2011) 3437–3447.

[103] A. Warshel, P.K. Sharma, M. Kato, W.W. Parson, Modeling electrostatic effects in proteins, Biochim. Biophys. Acta 1764 (2006) 1647–1676.

[104] W.M. Clark, Oxidation-Reduction Potentials on Organic Systems, Waverly Press, Baltimore, 1960.

[105] Z. Zhu, M.R. Gunner, Energetics of quinone-dependent electron and proton transfers in *Rhodobacter sphaeroides* photosynthetic reaction centers, Biochemistry 44 (2005) 82–96.

[106] A. Warshel, S.T. Russell, Calculations of electrostatic interactions in biological systems and in solutions, Q. Rev. Biophys. 17 (1984) 283–422.

[107] A.A. Rashin, B. Honig, Reevaluation of the Born model of ion hydration, J. Phys. Chem. 89 (1985) 5588–5593.

[108] M.R. Gunner, M.A. Saleh, E. Cross, A. ud-Doula, M. Wise, Backbone dipoles generate positive potentials in all proteins: origins and implications of the effect, Biophys. J. 78 (2000) 1126–1144.

[109] J. Kim, J. Mao, M.R. Gunner, Are acidic and basic groups in buried proteins predicted to be ionized? J. Mol. Biol. 348 (2005) 1283–1298.

[110] P.R. Rich, D.S. Bendall, A mechanism for the reduction of cytochromes by quinols in solution and its relevance to biological electron transfer reactions, FEBS Lett. 105 (1979) 189–194.

[111] R.C. Prince, P. Lloyd-Williams, J.M. Bruce, P.L. Dutton, Voltammetric measurements of quinones, Methods Enzymol. 125 (1986) 109–119.

[112] C.A. Wraight, Proton and electron transfer in the acceptor quinone complex of bacterial photosynthetic reaction centers, Front. Biosci. 9 (2004) 309–327.

[113] S. Berneche, B. Roux, Energetics of ion conduction through the K⁺ channel, Nature 414 (2001) 73–77.

[114] Y.Y. Sham, I. Muegge, A. Warshel, The effect of protein relaxation on charge–charge interactions and dielectric constant of proteins, Biophys. J. 74 (1998) 1744–1753.

[115] M.R. Gunner, X. Zhu, M.C. Klein, MCCE analysis of the pKas of introduced buried acids and bases in staphylococcal nuclease, Proteins 79 (2011) 3306–3319.

[116] H. Nakamura, T. Sakamoto, A. Wada, Dielectric of protein, Protein Eng. 2 (1988) 177–183.

[117] M.K. Gilson, B.H. Honig, The dielectric constant of a folded protein, Biopolymers 25 (1986) 2097–2119.

[118] L.I. Krishtalik, pH-dependent redox potential: how to use it correctly in the activation energy analysis, Biochim. Biophys. Acta 1604 (2003) 13–21.

[119] P. Sebban, P. Maroti, D.K. Hanson, Electron and proton transfer to the quinones in bacterial photosyntheic reaction centers: insight from combined approaches of molecular genetics and biophysics, Biochimie 77 (1995) 677–694.

[120] M.Y. Okamura, M.L. Paddock, M.S. Graige, G. Feher, Proton and electron transfer in bacterial reaction centers, Biochim. Biophys. Acta 1458 (2000) 148–163.

[121] W. Nitschke, A.W. Rutherford, Photosynthetic reaction centers: variations on a common structural theme? Trends Biochem. Sci. 16 (1991) 241–245.

[122] J.P. Allen, J.C. Williams, Photosynthetic reaction centers, FEBS Lett. 438 (1998) 5–9.

[123] M.L. Paddock, S.H. Rongey, G. Feher, M.Y. Okamura, Pathway of proton transfer in bacterial reaction centers: replacement of glutamic acid 212 in the L subunit by glutamine inhibits quinone (secondary acceptor) turnover, Proc. Natl. Acad. Sci. U. S. A. 86 (1989) 6602–6606.

[124] M.L. Paddock, A. Juth, G. Feher, M.Y. Okamura, Electrostatic effects of replacing Asp-L210 with Asn in bacterial RCs from *Rb. sphaeroides*, Biophys. J. 61 (1992) A153.

[125] M.L. Paddock, S.H. Rongey, P.H. McPherson, A. Juth, G. Feher, M.Y. Okamura, Pathway of proton transfer in bacterial reaction centers: role of aspartate-L213 in proton transfers associated with reduction of quinone to dihydroquinone, Biochemistry 33 (1994) 734–745.

[126] P. Maroti, D.K. Hanson, L. Baciou, S. Marianne, P. Sebban, Proton conduction within the reaction centers of *Rhodobacter capsulatus*: the electrostatic role of the protein, Proc. Natl. Acad. Sci. 91 (1994) 5617–5621.

[127] P. Sebban, P. Maroti, M. Schiffer, D.K. Hanson, Electrostatic dominoes: long distance propagation of mutational effects in photosynthetic reaction centers of *Rhodobacter capsulatus*, Biochemistry 34 (1995) 8390–8397.

[128] E. Takahashi, C.A. Wraight, A crucial role for Asp^{L213} in the proton transfer pathway to the secondary quinone of reaction centers from *Rhodobacter sphaeroides*, Biochim. Biophys. Acta 1020 (1990) 107–111.

[129] E. Takahashi, C.A. Wraight, Proton and electron transfer in the acceptor quinone complex of *Rhodobacter sphaeroides* reaction centers: characterization of site-directed mutants of the two ionizable residues, Glu L212 and Asp L213, in the Q$_B$ binding site, Biochemistry 31 (1992) 855–866.

[130] T.A. Wells, E. Takahashi, C.A. Wraight, Protein control of the redox potential of the primary quinone acceptor in reaction centers from *Rhodobacter sphaeroides*, Biochemistry 42 (2003) 4064–4074.

[131] P. Beroza, D.R. Fredkin, M.Y. Okamura, G. Feher, Electrostatic calculations of amino acid titration electron transfer, Q^-_AQ$_B$ → Q$_A$Q^-_B, in the reaction center, Biophys. J. 68 (1995) 2233–2250.

[132] B. Rabenstein, G.M. Ullmann, E.-W. Knapp, Calculation of protonation patterns in proteins with structural relaxation and molecular ensembles—application to the photosynthetic reaction center, Eur. Biophys. J. 27 (1998) 626–637.

[133] C.R.D. Lancaster, H. Michel, B. Honig, M.R. Gunner, Calculated coupling of electron and proton transfer in the photosynthetic reaction center of *Rhodopseudomonas viridis*, Biophys. J. 70 (1996) 2469–2492.

[134] E. Alexov, J. Miksovska, L. Baciou, M. Schiffer, D.K. Hanson, P. Sebban, M.R. Gunner, Modeling the effects of mutations on the free energy of the first electron transfer from Q^-_A to Q$_B$ in photosynthetic reaction centers, Biochemistry 39 (2000) 5940–5952.

[135] H. Ishikita, G. Morra, E.W. Knapp, Redox potential of quinones in photosynthetic reaction centers from *Rhodobacter sphaeroides*: dependence on protonation of Glu-L212 and Asp-L213, Biochemistry 42 (2003) 3882–3892.

[136] J. Madeo, M. Mihajlovic, T. Lazaridis, M.R. Gunner, Slow dissociation of a charged ligand: analysis of the primary quinone (Q$_A$) site of photosynthetic bacterial reaction centers, J. Am. Chem. Soc. 133 (2011) 17375–17385.

[137] B.A. Diner, C.C. Schenck, C. DeVitry, Effect of inhibitors, redox state and isoprenoid chain length on the affinity of ubiquinone for the secondary acceptor binding site in the reaction centers of photosynthetic bacteria, Biochim. Biophys. Acta 766 (1984) 9–20.

[138] J. Madeo, M.R. Gunner, Modeling binding kinetics at the Q$_A$ site in bacterial reaction centers, Biochemistry 44 (2005) 10994–11004.

[139] B.A. Diner, C. deVitry, J.-L. Popot, Quinone exchange in the Q$_A$ binding site of photosystem II reaction center core preparations isolated from *Chlamydomonas reinhardii*, Biochim. Biophys. Acta 934 (1988) 47–54.

[140] B.A. Diner, V. Petrouleas, J.J. Wendoloski, The iron-quinone electron–acceptor complex of photosystem II, Physiol. Plant. 81 (1991) 423–436.

[141] F.J.E. van Mieghem, W. Nitschke, P. Mathis, A.W. Rutherford, The influence of the quinone-iron electron acceptor complex on the reaction centre photochemistry of photosystem II, Biochim. Biophys. Acta 977 (1989) 207–214.

[142] C. Fufezan, C.M. Gross, M. Sjodin, A.W. Rutherford, A. Krieger-Liszkay, D. Kirilovsky, Influence of the redox potential of the primary quinone electron acceptor on photoinhibition in photosystem II, J. Biol. Chem. 282 (2007) 12492–12502.

[143] C.A. Wraight, The role of quinones in bacterial photosynthesis, Photochem. Photobiol. 30 (1979) 767–776.

[144] M.R. Gunner, P.L. Dutton, Temperature and $-\Delta G°$ dependence of the electron transfer from BPh^- to Q_A in reaction center protein from *Rhodobacter sphaeroides* with different quinones as Q_A, J. Am. Chem. Soc. 111 (1989) 3400–3412.

[145] N.W.T. Woodbury, W.W. Parson, Nanosecond fluorescence from isolated photosynthetic reaction centers from *Rhodopseudomonas sphaeroides*, Biochim. Biophys. Acta 767 (1984) 345–361.

[146] P. Maroti, C.A. Wraight, Flash-induced H^+ binding by bacterial photosynthetic reaction centers: influences of the redox states of the acceptor quinones and primary donor, Biochim. Biophys. Acta 934 (1988) 329–347.

[147] D. Kleinfeld, M.Y. Okamura, G. Feher, Electron transfer in reaction centers of *Rhodopseudomonas sphaeroides*: I. Determination of the charge recombination pathway of $D^+Q_AQ_B^-$ and free energy and kinetic relations between $Q_A^-Q_B$ and $Q_AQ_B^-$, Biochim. Biophys. Acta 766 (1984) 126–140.

[148] P.H. McPherson, M. Schonfeld, M.L. Paddock, M.Y. Okamura, G. Feher, Protonation and free energy changes associated with formation of QBH2 in native and Glu-L212 → Gln mutant reaction centers from *Rhodobacter sphaeroides*, Biochemistry 33 (1994) 1181–1193.

[149] P. Maróti, C.A. Wraight, The redox midpoint potential of the primary quinone of reaction centers in chromatophores of *Rhodobacter sphaeroides* is pH independent, Eur. Biophys. J. 37 (2008) 1207–1217.

[150] L.J. Mancino, D.P. Dean, R.E. Blankenship, Kinetics and thermodynamics of the $P870 + QA^- → P870 + QB^-$ reaction in isolated reaction centers from the photosynthetic bacterium *Rhodopseudomonas sphaeroides*, Biochim. Biophys. Acta 764 (1984) 46–54.

[151] D. Kleinfeld, M.Y. Okamura, G. Feher, Electron-transfer kinetics in photosynthetic reaction centers cooled to cryogenic temperatures in the charge separated state: evidence for light-induced structural changes, Biochemistry 23 (1984) 5780–5786.

[152] B.H. McMahon, J.D. Muller, C.A. Wraight, G.U. Nienhaus, Electron transfer and protein dynamics in the photosynthetic reaction center, Biophys. J. 74 (1998) 2567–2587.

[153] Q. Xu, L. Baciou, P. Sebban, M.R. Gunner, Exploring the energy landscape for Q_A^- to Q_B electron transfer in bacterial photosynthetic reaction centers: effect of substrate position and tail length on the conformational gating step, Biochemistry 41 (2002) 10021–10025.

[154] M.R. Gunner, J. Madeo, Z. Zhu, Modification of quinone electrochemistry by the proteins in the biological electron transfer chains: examples from photosynthetic reaction centers, J. Bioenerg. Biomembr. 40 (2008) 509–519.

[155] A. Futami, G. Hauska, Vectorial redox reactions of physiological quinones. II. A study of transient semiquinone formation, Biochim. Biophys. Acta 547 (1979) 597–608.

[156] W.J. Ingledew, T. Ohnishi, J.C. Salerno, Studies on a stabilisation of ubisemiquinone by *Escherichia coli* quinol oxidase, cytochrome bo, Eur. J. Biochem. 227 (1995) 903–908.

[157] G. Cecchini, E. Maklashina, V. Yankovskaya, T.M. Iverson, S. Iwata, Variation in proton donor/acceptor pathways in succinate:quinone oxidoreductases, FEBS Lett. 545 (2003) 31–38.

[158] C.R.D. Lancaster, Succinate: quinone oxidoreductases — what can we learn from *Wolinella succinogenes* quinol:fumarate reductase? FEBS Lett. 504 (2001) 133–141.

[159] H. Zhang, S.E. Chobot, A. Osyczka, C.A. Wraight, P.L. Dutton, C.C. Moser, Quinone and non-quinone redox couples in Complex III, J. Bioenerg. Biomembr. 40 (2008) 493–499.

[160] T. Ohnishi, S.T. Ohnishi, K. Shinzawa-Itoh, S. Yoshikawa, R.T. Weber, EPR detection of two protein-associated ubiquinone components (SQ(Nf) and SQ(Ns)) in the membrane in situ and in proteoliposomes of isolated bovine heart complex I, Biochim. Biophys. Acta 1817 (2012) 1803–1809.

[161] C.A. Wraight, Intraprotein proton transfer — concepts and realities from the bacterial photosynthetic reaction center, in: M. Wikström (Ed.), Biophysical and Structural Aspects of Bioenergetics, Royal Society of Chemistry, Cambridge, U.K., 2005, pp. 273–313.

[162] R.C. Prince, P.L. Dutton, J.M. Bruce, Electrochemistry of ubiquinones, menaquinones and plastoquinones in aprotic solvents, FEBS Lett. 160 (1983) 273–276.

[163] B.R. Eggins, J.Q. Chambers, Proton effects in electrochemistry of quinone hydroquinone system in aprotic solvents, J. Electrochem. Soc. 117 (1970) 186, (-&).

[164] D. Kleinfeld, M.Y. Okamura, G. Feher, Electron transfer in reaction centers of *Rhodopseudomonas sphaeroides*. II. Free energy and kinetic relations between the acceptor states $Q_A^-Q_B$ and $Q_AQ_B^{-2}$, Biochim. Biophys. Acta 809 (1985) 291–310.

[165] M.S. Graige, M.L. Paddock, G. Feher, M.Y. Okamura, Observation of the protonated semiquinone intermediate in isolated reaction centers from *Rhodobacter sphaeroides*: implications for the mechanism of electron and proton transfer in proteins, Biochemistry 38 (1999) 11465–11473.

[166] A. Vermeglio, R.K. Clayton, Kinetics of electron transfer between the primary and secondary electron acceptor in reaction centers from *Rhodoseudomonas sphaeroides*, Biochim. Biophys. Acta 461 (1977) 159–165.

[167] B.J. Hales, E.E. Case, Immobilized radicals IV. Biological semiquinone anions and neutral semiquinones, Biochim. Biophys. Acta 637 (1981) 291–302.

[168] G. Feher, R.A. Isaacson, M.Y. Okamura, W. Lubitz, ENDOR of semiquinones in reaction centers from *Rhodopseudomonas sphaeroides*, in: M.E. Michel-Beyerle (Ed.), Antennas and Reaction Centers of Photosynthetic Bacteria — Structure, Interactions and Dynamics, Springer-Verlag, Berlin, 1985, pp. 174–189.

[169] M.S. Graige, M.L. Paddock, J.M. Bruce, G. Feher, M.Y. Okamura, Mechanism of proton-coupled electron transfer for quinone (Q_B) reduction in reaction centers of *Rb. sphaeroides*, J. Am. Chem. Soc. 118 (1996) 9005–9016.

[170] B. Rabenstein, G.M. Ullmann, E.-W. Knapp, Energetics of electron-transfer and protonation reactions of the quinones in the photosynthetic reaction center of *Rhodopseudonas viridis*, Biochemistry 37 (1998) 2488–2495.

[171] H. Ishikita, E.W. Knapp, Variation of Ser-L223 hydrogen bonding with the Q_B redox state in reaction centers from *Rhodobacter sphaeroides*, J. Am. Chem. Soc. 126 (2004) 8059–8064.

[172] K.M. Giangiacomo, P.L. Dutton, In photosynthetic reaction centers, the free energy difference for electron transfer between quinones bound at the primary and secondary quinone-binding sites governs the observed secondary site specificity, Proc. Natl. Acad. Sci. U. S. A. 86 (1989) 2658–2662.

[173] A. Labahn, J.M. Bruce, M.Y. Okamura, G. Feher, Direct charge recombination from $D^+Q_AQ_B^-$ to DQ_AQ_B in bacterial reaction centers from *Rhodobacter sphaeroides* containing low potential quinone in the Q_A site, Chem. Phys. 97 (1995) 355–366.

[174] C.A. Wraight, A.S. Vakkasoglu, Y. Poluektov, A.J. Mattis, D. Nihan, B.H. Lipshutz, The 2-methoxy group of ubiquinone is essential for function of the acceptor quinones in reaction centers from *Rba. sphaeroides*, Biochim. Biophys. Acta 1777 (2008) 631–636.

[175] X. Zhang, M.R. Gunner, Affinity and activity of non-native quinones at the Q_B site of bacterial photosynthetic reaction centers, Photosynth. Res. (2013) (in press).

[176] Q. Xu, M.R. Gunner, Trapping conformational intermediate states in the reaction center protein from photosynthetic bacteria, Biochemistry 40 (2001) 3232–3241.

[177] Q. Xu, M.R. Gunner, Exploring the energy profile of the Q_A^- to Q_B electron transfer reaction in bacterial photosynthetic reaction centers: pH dependence of the conformational gating step, Biochemistry 41 (2002) 2694–2701.

[178] R. Hienerwadel, S. Grzybek, C. Fogel, W. Kreutz, M.Y. Okamura, M.L. Paddock, J. Breton, Protonation of Glu L212 following Q_B-formation in the photosynthetic reaction center of *Rhodobacter sphaeroides*: evidence from time-resolved infrared spectroscopy, Biochemistry 34 (1995) 2832–2843.

[179] E. Nabedryk, J. Breton, M.Y. Okamura, M.L. Paddock, Simultaneous replacement of Asp-L210 and Asp-M17 with Asn increases proton uptake by Glu-L212 upon first electron transfer to Q_B in reaction centers from *Rhodobacter sphaeroides*, Biochemistry 40 (2001) 13826–13832.

[180] A. Osyczka, C.C. Moser, P.L. Dutton, Fixing the Q cycle, Trends Biochem. Sci. 30 (2005) 176–182.

[181] J.L. Cape, M.K. Bowman, D.M. Kramer, Understanding the cytochrome bc complexes by what they don't do. The Q-cycle at 30, Trends Plant Sci. 11 (2006) 46–55.

[182] A.Y. Mulkidjanian, Activated Q-cycle as a common mechanism for cytochrome bc1 and cytochrome b6f complexes, Biochim. Biophys. Acta 1797 (2010) 1858–1868.

[183] W.A. Cramer, S.S. Hasan, E. Yamashita, The Q cycle of cytochrome bc complexes: a structure perspective, Biochim. Biophys. Acta 1807 (2011) 788–802.

[184] L. Kalman, J.C. Williams, J.P. Allen, Comparison of bacterial reaction centers and photosystem II, Photosynth. Res. 98 (2008) 643–655.

[185] M. Zheng, C. Dismukes, The conformation of the isoprenyl chain relative to the semiquinone head in the primary electron acceptor (Q_A) of the higher plant PSII (plastosemiquinone) differs from that in bacterial reaction centers (ubisemiquinone or menasemiquinone) by ca. 90°, Biochemistry 35 (1996) 8955–8963.

[186] H.A. Frank, G.W. Brudvig, Redox functions of carotenoids in photosynthesis, Biochemistry 43 (2004) 8607–8615.

[187] P. Pospisil, Enzymatic function of cytochrome b559 in photosystem II, J. Photochem. Photobiol. B 104 (2011) 341–347.

[188] H. Ishikita, E.-W. Knapp, Redox potentials of chlorophylls and b-carotene in the antenna complexes of photosystem II, J. Am. Chem. Soc. 127 (2005) 1963–1968.

[189] I. Saitoh, H. Miyoshi, R. Shimizu, H. Iwamura, Comparison of structure of quinone redox site in the mitochondrial cytochrome-bc1 complex and photosystem II (Q_B site), Eur. J. Biochem. 209 (1992) 73–79.

[190] A.W. Rutherford, W. Nitschke, Photosystem II and the quinone–iron containing reaction centers: comparisons and evolutionary perspectives, in: H. Baltscheffsky (Ed.), Origin and Evolution of Biological Energy Conversion, VCH, New York, 1996, pp. 143–175.

[191] F. Rappaport, M. Guergova-Kuras, P.J. Nixon, B.A. Diner, J. Lavergne, Kinetics and pathways of charge recombination in photosystem II, Biochemistry 41 (2002) 8518–8527.

[192] F. Muh, C. Glockner, J. Hellmich, A. Zouni, Light-induced quinone reduction in photosystem II, Biochim. Biophys. Acta 1817 (2012) 44–65.

[193] B.A. Diner, F. Rappaport, Structure, dynamics, and energetics of the primary photochemistry of photosystem II of oxygenic photosynthesis, Annu. Rev. Plant Biol. 53 (2002) 551–580.

[194] J. Wachtveitl, J.W. Farchaus, R. Das, M. Lutz, B. Robert, T.A. Mattioli, Structure, spectroscopic, and redox properties of *Rhodobacter sphaeroides* reaction centers bearing point mutations near the primary electron donor, Biochemistry 32 (1993) 12875–12886.

[195] F. Rappaport, B.A. Diner, Primary photochemistry and energetics leading to the oxidation of the Mn_4Ca cluster and to the evolution of molecular oxygen in photosystem II, Coord. Chem. Rev. 252 (2008) 259–272.

[196] R. Hill, F. Bendall, Function of the two cytochrome components in chloroplasts: a working hypothesis, Nature 186 (1960) 136–137.

[197] R.C. Prince, Photosynthesis: the Z-scheme revised, Trends Biochem. Sci. 21 (1996) 121–122.

[198] D.A. Walker, The Z-scheme—down hill all the way, Trends Plant Sci. 7 (2002) 183–185.

[199] R.E. Blankenship, D.M. Tiede, J. Barber, G.W. Brudvig, G. Fleming, M. Ghirardi, M.R. Gunner, W. Junge, D.M. Kramer, A. Melis, T.A. Moore, C.C. Moser, D.G. Nocera, A.J. Nozik, D.R. Ort, W.W. Parson, R.C. Prince, R.T. Sayre, Comparing photosynthetic and photovoltaic efficiencies and recognizing the potential for improvement, Science 332 (2011) 805–809.

[200] Y. Pushkar, J. Yano, P. Glatzel, J. Messinger, A. Lewis, K. Sauer, U. Bergmann, V. Yachandra, Structure and orientation of the Mn_4Ca cluster in plant photosystem II membranes studied by polarized range-extended X-ray absorption spectroscopy, J. Biol. Chem. 282 (2007) 7198–7208.

[201] J. Barber, J.W. Murray, The structure of the Mn_4Ca^{2+} cluster of photosystem II and its protein environment as revealed by X-ray crystallography, Phil. Trans. R. Soc. B 363 (2008) 1129–1137.

[202] A.M. Hays, I.R. Vassiliev, J.H. Golbeck, R.J. Debus, Role of D1-His190 in proton-coupled electron transfer reactions in photosystem II: a chemical complementation study, Biochemistry 37 (1998) 11352–11365.

[203] H. Matsuoka, J.R. Shen, A. Kawamori, K. Nishiyama, Y. Ohba, S. Yamauchi, Proton-coupled electron-transfer processes in photosystem II probed by highly resolved g-anisotropy of redox-active tyrosine YZ, J. Am. Chem. Soc. 133 (2011) 4655–4660.

[204] P.G. Falkowski, Y. Isozaki, Geology. The story of O_2, Science 322 (2008) 540–542.

[205] M.F. Hohmann-Marriott, R.E. Blankenship, Evolution of photosynthesis, Annu. Rev. Plant Biol. 62 (2011) 515–548.

[206] J.P. Allen, J.C. Williams, The evolutionary pathway from anoxygenic to oxygenic photosynthesis examined by comparison of the properties of photosystem II and bacterial reaction centers, Photosynth. Res. 107 (2011) 59–69.

[207] B. Kok, B. Forbush, M. McGloin, Cooperation of charges in photosynthetic O_2 evolution—I. A linear four step mechanism, Photochem. Photobiol. 11 (1970) 457–475.

[208] M. Haumann, C. Mueller, P. Liebisch, L. Iuzzolino, J. Dittmer, M. Grabolle, T. Neisius, W. Meyer-Klaucke, H. Dau, Structural and oxidation state changes of the photosystem II manganese complex in four transitions of the water oxidation cycle $(S0 \to S1, S1 \to S2, S2 \to S3, and S3,4 \to S0)$ characterized by X-ray absorption spectroscopy at 20 K and room temperature, Biochemistry 44 (2005) 1894–1908.

[209] I. McConnell, G. Li, G.W. Brudvig, Energy conversion in natural and artificial photosynthesis, Chem. Biol. 17 (2010) 434–447.

[210] L. Iuzzolino, J. Dittmer, W. Doerner, W. Meyer-Klaucke, H. Dau, X-ray absorption spectroscopy on layered photosystem II membrane particles suggests manganese-centered oxidation of the oxygen-evolving complex for the S0–S1, S1–S2, and S2–S3 transitions of the water oxidation cycle, Biochemistry 37 (1998) 17112–17119.

[211] B.A. Barry, G.T. Babcock, Tyrosine radicals are involved in the photosynthetic oxygen-evolving system, Proc. Natl. Acad. Sci. U. S. A. 84 (1987) 7099–7103.

[212] C. Tommos, G.T. Babcock, Proton and hydrogen currents in photosynthetic water oxidation, Biochim. Biophys. Acta 1458 (2000) 199–219.

[213] G.W. Brudvig, Water oxidation chemistry of photosystem II, Philos. Trans. R. Soc. Lond. B Biol. Sci. 363 (2008) 1211–1218, (discussion 1218–1219).

[214] B.A. Barry, J. Chen, J. Keough, D. Jenson, A. Offenbacher, C. Pagba, Proton coupled electron transfer and redox active tyrosines: structure and function of the tyrosyl radicals in ribonucleotide reductase and photosystem II, J. Phys. Chem. Lett. 3 (2012) 543–554.

[215] W.T. Dixon, D. Murphy, Determination of the acidity constants of some phenol radical cations by means of electron spin resonance, J. Chem. Soc. Faraday Trans. 72 (1972).

[216] F. Rappaport, A. Boussac, D.A. Force, J. Peloquin, M. Brynda, M. Sugiura, S. Un, R.D. Britt, B.A. Diner, Probing the coupling between proton and electron transfer in photosystem II core complexes containing a 3-fluorotyrosine, J. Am. Chem. Soc. 131 (2009) 4425–4433.

[217] M.C. Martínez-Rivera, B.W. Berry, K.G. Valentine, K. Westerlund, S. Hay, C. Tommos, Electrochemical and structural properties of a protein system designed to generate tyrosine pourbaix diagrams, J. Am. Chem. Soc. 133 (2011) 17786–17795.

[218] R.J. Williams, The natural selection of the chemical elements, Cell. Mol. Life Sci. 53 (1997) 816–829.

[219] C.S. Babu, T. Dudev, R. Casareno, J.A. Cowan, C. Lim, A combined experimental and theoretical study of divalent metal ion selectivity and function in proteins: application to *E. coli* ribonuclease H1, J. Am. Chem. Soc. 125 (2003) 9318–9328.

[220] T. Dudev, C. Lim, Principles governing Mg, Ca, and Zn binding and selectivity in proteins, Chem. Rev. 103 (2003) 773–788.

[221] T. Dudev, L.Y. Chang, C. Lim, Factors governing the substitution of La^{3+} for Ca^{2+} and Mg^{2+} in metalloproteins: a DFT/CDM study, J. Am. Chem. Soc. 127 (2005) 4091–4103.

[222] T. Dudev, C. Lim, Metal binding affinity and selectivity in metalloproteins: insights from computational studies, Annu. Rev. Biophys. 37 (2008) 97–116.

[223] T. Dudev, C. Lim, Metal-binding affinity and selectivity of nonstandard natural amino acid residues from DFT/CDM calculations, J. Phys. Chem. B 113 (2009) 11754–11764.

[224] T. Dudev, C. Lim, Competition among Ca^{2+}, Mg^{2+}, and Na^+ for model ion channel selectivity filters: determinants of ion selectivity, J. Phys. Chem. B 116 (2012) 10703–10714.

[225] F.A. Armstrong, Why did nature choose manganese to make oxygen? Philos. Trans. R. Soc. Lond. B Biol. Sci. 363 (2008) 1263–1270, (discussion 1270).

[226] R.J. Pace, R. Stranger, S. Petrie, Why nature chose Mn for the water oxidase in photosystem II, Dalton Trans. 41 (2012) 7179–7189.

[227] V.C. Culotta, M. Yang, T.V. O'Halloran, Activation of superoxide dismutases: putting the metal to the pedal, Biochim. Biophys. Acta 1763 (2006) 747–758.

[228] A.F. Miller, Redox tuning over almost 1 V in a structurally conserved active site: lessons from Fe-containing superoxide dismutase, Acc. Chem. Res. 41 (2008) 501–510.

[229] A.F. Miller, K. Padmakumar, D.L. Sorkin, A. Karapetian, C.K. Vance, Proton-coupled electron transfer in Fe-superoxide dismutase and Mn-superoxide dismutase, J. Inorg. Biochem. 93 (2003) 71–83.

[230] J.L. Zimmermann, A.W. Rutherford, EPR studies of the oxygen-evolving enzyme of photosystem II, Biochim. Biophys. Acta Bioenerg. 767 (1984) 160–167.

[231] J.L. Zimmermann, A.W. Rutherford, Electron paramagnetic resonance properties of the S2 state of the oxygen-evolving complex of photosystem II, Biochemistry 25 (1986) 4609–4615.

[232] J.P. McEvoy, G.W. Brudvig, Water-splitting chemistry of photosystem II, Chem. Rev. 106 (2006) 4455–4483.

[233] G.J. Yeagle, M.L. Gilchrist, R.M. McCarrick, R.D. Britt, Multifrequency pulsed electron paramagnetic resonance study of the S-2 state of the photosystem II manganese cluster, Inorg. Chem. 47 (2008) 1803–1814.

[234] M. Dudev, J. Wang, T. Dudev, C. Lim, Factors governing the metal coordination number in metal complexes from Cambridge Structural Database analyses, J. Phys. Chem. B 110 (2006) 1889–1895.

[235] T. Dudev, C. Lim, Competition between protein ligands and cytoplasmic inorganic anions for the metal cation: a DFT/CDM study, J. Am. Chem. Soc. 128 (2006) 10541–10548.

[236] T. Dudev, C. Lim, A DFT/CDM study of metal-carboxylate interactions in metalloproteins: factors governing the maximum number of metal-bound carboxylates, J. Am. Chem. Soc. 128 (2006) 1553–1561.

[237] D.T. Richens, The Chemistry of Aqua Ions, John Wiley and Sons, Sussex, 1997.

[238] J.L. Dempsey, J.R. Winkler, H.B. Gray, Proton-coupled electron flow in protein redox machines, Chem. Rev. 110 (2010) 7024–7039.

[239] M.H. Huynh, T.J. Meyer, Proton-coupled electron transfer, Chem. Rev. 107 (2007) 5004–5064.

[240] M.J. Baldwin, A. Gelasco, V.L. Pecoraro, The effect of protonation on $[Mn(IV)(\mu-O)]_2$ complexes, Photosynth. Res. 38 (1993) 303–308.

[241] M.J. Baldwin, V.L. Pecoraro, Energetics of proton-coupled electron transfer in high-valent $Mn_2(\mu-O)_2$ systems: models for water oxidation by the oxygen-evolving complex of photosystem II, J. Am. Chem. Soc. 118 (1996) 11325.

[242] C.W. Cady, R.H. Crabtree, G.W. Brudvig, Functional models for the oxygen-evolving complex of photosystem II, Coord. Chem. Rev. 252 (2008) 444–455.

[243] H.H. Thorp, J.E. Sarneski, G.W. Brudvig, R.H. Crabtree, Proton-coupled electron transfer in $[(bpy)_2Mn(\mu-O)_2Mn(bpy)_2]^{3+}$, J. Am. Chem. Soc. 111 (1989) 9249–9250.

[244] M.T. Caudle, V.L. Pecoraro, Thermodynamic viability of hydrogen atom transfer from water coordinated to the oxygen-evolving complex of photosystem II, J. Am. Chem. Soc. 119 (1997) 3415–3416.

[245] S. Kristjánsdóttir, J. Norton, Acidity of hydrido transition metal complexes in solution, in: A. Dedieu (Ed.), Transition Metal Hydrides, VCH Publishers, 1992, pp. 309–359.

[246] M. Amin, L. Vogt, S. Vassiliev, I. Rivalta, D. Bruce, G.W. Brudvig, V.S. Batista, M.R. Gunner, A simple classical model to study high-valent oxomanganese model complexes and their relevance to the oxygen evolving complex of photosystem II, J. Phys. Chem B. (2013), http://dx.doi.org/10.1021/jp403321b.

[247] A. Galstyan, A. Robertazzi, E.W. Knapp, Oxygen-evolving Mn cluster in photosystem II: the protonation pattern and oxidation state in the high-resolution crystal structure, J. Am. Chem. Soc. 134 (2012) 7442–7449.

[248] J. Limburg, J.S. Vrettos, L.M. Liable-Sands, A.L. Rheingold, R.H. Crabtree, G.W. Brudvig, A functional model for O–O bond formation by the O_2-evolving complex in photosystem II, Science 283 (1999) 1524–1527.

[249] J.P. McEvoy, J.A. Gascon, E.M. Sproviero, V.S. Batista, G.W. Brudvig, Computational structural model of the oxygen evolving complex in photosystem II: complete ligation by protein, water and chloride, in: D. Bruce, A. van der Est (Eds.), Photosynthesis: Fundamental Aspects to Global Perspectives, Allen Press, Lawrence, Kansas, 2005, pp. 278–280.

[250] E.M. Sproviero, J.A. Gascon, J.P. McEvoy, G.W. Brudvig, V.S. Batista, QM/MM models of the O_2-evolving complex of photosystem II, J. Chem. Theory Comput. 2 (2006) 1119–1134.

[251] E.M. Sproviero, J.A. Gascon, J.P. McEvoy, G.W. Brudvig, V.S. Batista, Quantum mechanics/molecular mechanics structural models of the oxygen-evolving complex of photosystem II, Curr. Opin. Struct. Biol. 17 (2007) 173–180.

[252] E.M. Sproviero, J.A. Gascon, J.P. McEvoy, G.W. Brudvig, V.S. Batista, QM/MM study of the catalytic cycle for water splitting in photosystem II, J. Am. Chem. Soc. 130 (2008) 3428–3442.

[253] E.M. Sproviero, J.A. Gascon, J.P. McEvoy, G.W. Brudvig, V.S. Batista, Computational insights into the oxygen-evolving complex of photosystem II, Photosynth. Res. 97 (2008).

[254] K. Roos, P.E. Siegbahn, A comparison of two-electron chemistry performed by the manganese and iron heterodimer and homodimers, J. Biol. Inorg. Chem. 17 (2012) 363–373.

[255] S.L. Chen, M.R. Blomberg, P.E. Siegbahn, How is methane formed and oxidized reversibly when catalyzed by Ni-containing methyl-coenzyme M reductase? Chemistry 18 (2012) 6309–6315.

[256] T. Borowski, A. Wojcik, A. Milaczewska, V. Georgiev, M.R. Blomberg, P.E. Siegbahn, The alkenyl migration mechanism catalyzed by extradiol dioxygenases: a hybrid DFT study, J. Biol. Inorg. Chem. 17 (2012) 881–890.

[257] P.E.M. Siegbahn, Water oxidation in photosystem II: oxygen release, proton release and the effect of chloride, Dalton Trans. (2009) 10063–10068.

[258] B. Brena, P.E. Siegbahn, H. Agren, Modeling near-edge fine structure X-ray spectra of the manganese catalytic site for water oxidation in photosystem II, J. Am. Chem. Soc. 134 (2012) 17157–17167.

[259] P.E.M. Siegbahn, M. Lundberg, The mechanism for dioxygen formation in PSII studied by quantum chemical methods, Photochem. Photobiol. Sci. 4 (2005) 1035–1043.

[260] P.E.M. Siegbahn, M. Lundberg, Hydroxide instead of bicarbonate in the structure of the oxygen evolving complex, J. Inorg. Biochem. 100 (2006) 1035–1040.

[261] S. Luber, I. Rivalta, Y. Umena, K. Kawakami, J.R. Shen, N. Kamiya, G.W. Brudvig, V.S. Batista, S1-state model of the O_2-evolving complex of photosystem II, Biochemistry 50 (2011) 6308–6311.

[262] W. Ames, D.A. Pantazis, V. Krewald, N. Cox, J. Messinger, W. Lubitz, F. Neese, Theoretical evaluation of structural models of the S2 state in the oxygen evolving complex of photosystem II: protonation states and magnetic interactions, J. Am. Chem. Soc. 133 (2011) 19743–19757.

[263] P.E. Siegbahn, Water oxidation mechanism in photosystem II, including oxidations, proton release pathways, O–O bond formation and O_2 release, Biochim. Biophys. Acta (2012) (Electronic publication ahead of print).

[264] S. Milikisiyants, R. Chatterjee, A. Weyers, A. Meenaghan, C. Coates, K.V. Lakshmi, Ligand environment of the S2 state of photosystem II: a study of the hyperfine interactions of the tetranuclear manganese cluster by 2D 14 N HYSCORE spectroscopy, J. Phys. Chem. B 114 (2010) 10905–10911.

[265] H. Suzuki, M. Sugiura, T. Noguchi, Monitoring proton release during photosynthetic water oxidation in photosystem II by means of isotope-edited infrared spectroscopy, J. Am. Chem. Soc. 131 (2009) 7849–7857.

[266] P. Jahns, W. Junge, Proton release during the four steps of photosynthetic water oxidation: induction of 1:1:1:1 pattern due to lack of chlorophyll a/b binding proteins, Biochemistry 31 (1992) 7398–7403.

[267] I. Rivalta, M. Amin, S. Luber, S. Vassiliev, R. Pokhrel, Y. Umena, K. Kawakami, J.R. Shen, N. Kamiya, D. Bruce, G.W. Brudvig, M.R. Gunner, V.S. Batista, Structural-functional role of chloride in photosystem II, Biochemistry 50 (2011) 6312–6315.

[268] J. Baudry, E. Tajkhorshid, F. Molnar, J. Phillips, K. Schulten, Molecular dynamics study of bacteriorhodopsin and the purple membrane, J. Phys. Chem. B 105 (2001) 905–918.

[269] M. Clemens, P. Phatak, Q. Cui, A.N. Bondar, M. Elstner, Role of Arg82 in the early steps of the bacteriorhodopsin proton-pumping cycle, J. Phys. Chem. B 115 (2011) 7129–7135.

[270] H. Luecke, B. Schobert, H.T. Richter, J.P. Cartailler, J.K. Lanyi, Structural changes in bacteriorhodopsin during ion transport at 2 Ångstrom resolution, Science 286 (1999) 255–261.

[271] H. Luecke, B. Schobert, H.T. Richter, J.P. Cartailler, J.K. Lanyi, Structure of bacteriorhodopsin at 1.55 A resolution, J. Mol. Biol. 291 (1999) 899–911.

[272] R. Callendar, H. Deng, Nonresonance Raman difference spectroscopy, Annu. Rev. Biophys. Biomol. Struct. 23 (1994) 215–245.

[273] K. Gerwert, B. Hess, J. Soppa, D. Oesterhelt, Role of aspartate-96 in proton translocation by bacteriorhodopsin, Proc. Natl. Acad. Sci. U. S. A. 86 (1989) 4943–4947.

[274] B. Hessling, J. Herbst, R. Rammelsberg, K. Gerwert, Fourier transform infrared double-flash experiments resolve bacteriorhodopsin's M1 to M2 transition, Biophys. J. 73 (1997) 2071–2080.

[275] R. Rammelsberg, G. Huhn, M. Lubben, K. Gerwert, Bacteriorhodopsin's intramolecular proton-release pathway consists of a hydrogen-bonded network, Biochemistry 37 (1998) 5001–5009.

[276] N. Radzwill, K. Gerwert, H.J. Steinhoff, Time-resolved detection of transient movement of helices F and G in doubly spin-labeled bacteriorhodopsin, Biophys. J. 80 (2001) 2856–2866.

[277] E. Freier, S. Wolf, K. Gerwert, Proton transfer via a transient linear water-molecule chain in a membrane protein, Proc. Natl. Acad. Sci. U. S. A. 108 (2011) 11435–11439.

[278] J.K. Lanyi, Bacteriorhodopsin, Biochim. Biophys. Acta 1460 (2000) 1–3.

[279] T. Hirai, S. Subramaniam, Structural insights into the mechanism of proton pumping by bacteriorhodopsin, FEBS Lett. 545 (2003) 2–8.

[280] S. Szaraz, D. Oesterhelt, P. Ormos, pH-induced structural-changes in bacteriorhodopsin studied by Fourier-transform infrared-spectroscopy, Biophys. J. 67 (1994) 1706–1712.

[281] S.P. Balashov, T.G. Ebrey, Trapping and spectroscopic identification of the photointermediates of bacteriorhodopsin at low temperatures, Photochem. Photobiol. 73 (2001) 453–462.

[282] J.K. Lanyi, S.P. Balashov, Xanthorhodopsin: a bacteriorhodopsin-like proton pump with a carotenoid antenna, Biochim. Biophys. Acta 1777 (2008) 684–688.

[283] F. Garczarek, L.S. Brown, J.K. Lanyi, K. Gerwert, Proton binding within a membrane protein by a protonated water cluster, Proc. Natl. Acad. Sci. U. S. A. 102 (2005) 3633–3638.

[284] V.Z. Spassov, H. Luecke, K. Gerwert, D. Bashford, pK_a calculations suggest storage of an excess proton in a hydrogen-bonded water network in bacteriorhodopsin, J. Mol. Biol. 312 (2001) 203–219.

[285] A.N. Bondar, M. Elstner, S. Suhai, J.C. Smith, S. Fischer, Mechanism of primary proton transfer in bacteriorhodopsin, Structure 12 (2004) 1281–1288.

[286] G. Mathias, D. Marx, Structures and spectral signatures of protonated water networks in bacteriorhodopsin, Proc. Natl. Acad. Sci. U. S. A. 104 (2007) 6980–6985.

[287] Y. Xiao, M.S. Hutson, M. Belenky, J. Herzfeld, M.S. Braiman, Role of arginine-82 in fast proton release during the bacteriorhodopsin photocycle: a time-resolved FT-IR study of purple membranes containing ^{15}N-labeled arginine, Biochemistry 43 (2004) 12809–12818.

[288] B. Schobert, L.S. Brown, J.K. Lanyi, Crystallographic structures of the M and N intermediates of bacteriorhodopsin: assembly of a hydrogen-bonded chain of water molecules between Asp-96 and the retinal Schiff base, J. Mol. Biol. 330 (2003) 553–570.

[289] H.T. Richter, L.S. Brown, R. Needleman, J.K. Lanyi, A linkage of the pka's of asp-85 and glu-204 forms part of the reprotonation switch of bateriorhodopsin, Biochemistry 35 (1996) 4054–4062.

[290] R.B. Gennis, Coupled proton and electron transfer reactions in cytochrome oxidase, Front. Biosci. 9 (2004) 581–591.

[291] M.R. Blomberg, P.E. Siegbahn, The mechanism for proton pumping in cytochrome c oxidase from an electrostatic and quantum chemical perspective, Biochim. Biophys. Acta 1817 (2012) 495–505.

[292] V.Y. Artzatbanov, A.A. Konstantinov, V.P. Skulachev, Involvement of intramitochondrial protons in redox reactions of cytochrome alpha, FEBS Lett. 87 (1978) 180–185.

[293] M.H.B. Stowell, T.M. McPhillips, D.C. Rees, S.M. Soltis, E. Abresch, G. Feher, Light-induced structural changes in photosynthetic reaction center: implications for mechanism of electron-proton transfer, Science 276 (1997) 812–816.

[294] R.H.G. Baxter, N. Ponomarenko, V. Srajer, R. Pahl, K. Moffat, J.R. Norris, Time-resolved crystallographic studies of light-induced structural changes in the photosynthetic reaction centers, Proc. Natl. Acad. Sci. U. S. A. 101 (2004) 5982–5987.

[295] R.H.G. Baxter, B.-L. Seagle, N. Ponomarenko, J.R. Norris, Cryogenic structure of the photosynthetic reaction center of *Blastochloris viridis* in the light and dark, Acta Crystallogr. D61 (2005) 605–612.

[296] S. Boutet, L. Lomb, G.J. Williams, T.R. Barends, A. Aquila, R.B. Doak, U. Weierstall, D.P. DePonte, J. Steinbrener, R.L. Shoeman, M. Messerschmidt, A. Barty, T.A. White, S. Kassemeyer, R.A. Kirian, M.M. Seibert, P.A. Montanez, C. Kenney, R. Herbst, P. Hart, J. Pines, G. Haller, S.M. Gruner, H.T. Philipp, M.W. Tate, M. Hromalik, L.J. Koerner, N. van Bakel, J. Morse, W. Ghonsalves, D. Arnlund, M.J. Bogan, C. Caleman, R. Fromme, C.Y. Hampton, M.S. Hunter, L.C. Johansson, G. Katona, C. Kupitz, M. Liang, A.V. Martin, K. Nass, L. Redecke, F. Stellato, N. Timneanu, D. Wang, N.A. Zatsepin, D. Schafer, J. Defever, R. Neutze, P. Fromme, J.C. Spence, H.N. Chapman, I. Schlichting, High-resolution protein structure determination by serial femtosecond crystallography, Science 337 (2012) 362–364.

[297] D.A. Proshlyakov, M.A. Pressler, C. Demaso, J.F. Leykam, D.L. Dewitt, G.T. Babcock, Oxygen activation and reduction in respiration involvement of redox-active tyrosine 244, Science 290 (2000) 1588–1591.

[298] C.W. Hoganson, M.A. Pressler, D.A. Proshlyakov, G.T. Babcock, From water to oxygen and back again: mechanistic similarities in the enzymatic redox conversions between water and dioxygen, Biochim. Biophys. Acta 1365 (1998) 170–174.

[299] G. Babcock, How oxygen is activated and reduced in respiration, Proc. Natl. Acad. Sci. U. S. A. 96 (1999) 12971–12973.

[300] T.P. Silverstein, Photosynthetic water oxidation vs. mitochondrial oxygen reduction: distinct mechanistic parallels, J. Bioenerg. Biomembr. 43 (2011) 437–446.

[301] H. Michel, Cytochrome c oxidase: catalytic cycle and mechanisms of proton pumping—a discussion, Biochemistry 38 (1999) 15129–15140.

[302] M. Wikstrom, Proton translocation by cytochrome c oxidase a rejoiner to recent criticism, J. Am. Chem. Soc. 39 (2000) 3515–3519.

[303] M. Wikstrom, M.I. Verkhovsky, Proton translocation by cytochrome c oxidase in different phases of the catalytic cycle, Biochim. Biophys. Acta 1555 (2002) 128–132.

[304] H. Michel, The mechanism of proton pumping by cytochrome c oxidase, Proc. Natl. Acad. Sci. U. S. A. 95 (1998) 12819–12824.

[305] I. Belevich, D.A. Bloch, N. Belevich, M. Wikström, M.I. Verkhovsky, Exploring the proton pump mechanism of cytochrome c oxidase in real time, Proc. Natl. Acad. Sci. U. S. A. 104 (2007) 2685–2690.

[306] I. Belevich, M.I. Verkhovsky, M. Wikström, Proton-coupled electron transfer drives the proton pump of cytochrome c oxidase, Nature 440 (2006) 829–832.

[307] E.A. Gorbikova, M. Wikstrom, M.I. Verkhovsky, The protonation state of the cross-linked tyrosine during the catalytic cycle of cytochrome c oxidase, J. Biol. Chem. 283 (2008) 34907–34912.

[308] C.J. Reedy, B.R. Gibney, Heme protein assemblies, Chem. Rev. 104 (2004) 617–649.

[309] M.R. Gunner, B. Honig, Electrostatic analysis of the midpoints of the four hemes in the bound cytochrome of the reaction center of Rp. viridis, in: J. Jortner, B. Pullman (Eds.), Perspectives in Photosynthesis: Proceedings of the Twenty-Second Jerusalem Symposium on Quantum Chemistry and Biochemistry, Kluwer Academic Publisher, Dordrecht, 1990, pp. 53–60.

[310] O.Q. Munro, H.M. Marques, Heme-peptide models for hemoproteins. 1. Solution chemistry of N-acetylmicroperoxidase-8, Inorg. Chem. 35 (1996) 3752–3767.

[311] O.Q. Munro, H.M. Marques, Heme-peptide models for hemoproteins. 2. N-Acetylmicroperoxidase-8: Study of the π–π dimers formed at high ionic strength using a modified version of molecular exciton theory, Inorg. Chem. 35 (1996) 3768–3779.

[312] H.M. Marques, O.Q. Munro, T. Munro, M. de Wet, P.R. Vashi, Coordination of N-donor ligands by the monomeric ferric porphyrin N-acetylmicroperoxidase-8, Inorg. Chem. 38 (1999) 2312–2319.

[313] H.M. Marques, I. Cukrowski, P.R. Vashi, Co-ordination of weak field ligands by N-acetylmicroperoxidase-8 (NAcMP8), a ferric haempeptide from cytochrome c, and the influence of the axial ligand on the reduction potential of complexes of NAcMP8, J. Chem. Soc. 2000 (2000) 1335–1342.

[314] P.R. Vashi, H.M. Marques, The coordination of imidazole and substituted pyridines by the hemeoctapeptide N-acetyl-ferromicroperoxidase-8 (Fe^{II}NAcMP8), J. Inorg. Biochem. 98 (2004) 1471–1482.

[315] R. Santucci, H. Reinhard, M. Brunori, Direct electrochemistry of the undacapeptide from cytochrome c (microperoxidase) at a glassy carbon electrode, J. Am. Chem. Soc. 110 (1988) 8536–8537.

[316] Y. Song, J. Mao, M.R. Gunner, Electrostatic environment of hemes in proteins: pK$_a$s of hydroxyl ligands, Biochemistry 45 (2006) 7949–7958.

[317] S. Jeon, T.C. Bruice, Electrochemical potentials and associated pK$_a$ values for the various oxidation states of a water-soluble, non μ-oxo dimer forming chromium tetraphenylporphyrin in aqueous solution, Inorg. Chem. 30 (1991) 4311–4315.

[318] S. Jeon, T.C. Bruice, Redox chemistry of water-soluble iron, manganese, and chromium metalloporphyrins and acid–base behavior of their lyate axial ligands in aqueous solution: influence of electronic effects, Inorg. Chem. 31 (1992) 4843–4848.

[319] R.K. Behan, M.T. Green, On the status of ferryl protonation, J. Inorg. Biochem. 100 (2006) 448–459.

[320] M.T. Green, Application of Badger's rule to heme and non-heme iron–oxygen bonds: an examination of ferryl protonation states, J. Am. Chem. Soc. 128 (2006) 1902–1906.

[321] G.T. Babcock, B.A. Barry, R.J. Debus, C.W. Hoganson, M. Atamian, L. McIntosh, I. Sithole, C.F. Yocum, Water oxidation in photosystem II: from radical chemistry to multielectron chemistry, Biochemistry 28 (1989) 9557–9565.

[322] F. MacMillan, A. Kannt, J. Behr, T. Prisner, H. Michel, Direct evidence for a tyrosine radical in the reaction of cytochrome c oxidase with hydrogen peroxide, Biochemistry 38 (1999) 9179–9184.

[323] R. Richarz, K. Wüthrich, Carbon-13 NMR chemical shifts of the common amino acid residues measured in aqueous solutions of the linear tetrapeptides H-Gly-Gly-X-L-Ala-OH, Biopolymers 17 (1975) 2133–2141.

[324] K.M. McCauley, J.M. Vrtis, J. Dupont, W.A. van der Donk, Insights into the functional role of the tyrosine–histidine linkage in cytochrome c oxidase, J. Am. Chem. Soc. 122 (2000) 2403–2404.

[325] A. Jasaitis, M.I. Verkhovsky, J.E. Morgan, M.L. Verkhovskaya, M. Wikstom, Assignment and charge translocation stoichiometries of the major electrogenic phases in the reaction of cytochrome c oxidase with dioxygen, Biochemistry 38 (1999) 2697–2706.

[326] K. Faxen, G. Gilderson, P. Adelroth, P. Brzezinski, A mechanistic principle for proton pumping by cytochrome c oxidase, Nature 437 (2005) 286–289.

[327] M. Wikstrom, M.I. Verkhovsky, Towards the mechanism of proton pumping by the haem-copper oxidases, Biochim. Biophys. Acta 1757 (2006) 1047–1051.

[328] S. Jünemann, B. Meunier, R.B. Gennis, P.R. Rich, Effects of mutation of the conserved lysine-362 in cytochrome c oxidase from Rhodobacter sphaeroides, Biochemistry 36 (1997) 14456–14464.

[329] A.A. Konstantinov, S. Siletsky, D. Mitchell, A. Kaulen, R.B. Gennis, The roles of the two proton input channels in cytochrome c oxidase from Rhodobacter sphaeroides probed by the effects of site-directed mutations on time-resolved electrogenic intraprotein proton transfer, Proc. Natl. Acad. Sci. U. S. A. 94 (1997) 9085–9090.

[330] D. Zaslavsky, R.B. Gennis, Substitution of lysine-362 in a putative proton-conducting channel in the cytochrome c oxidase from Rhodobacter

[331] J.A. Halfen, J.J. Bodwin, V.L. Pecoraro, Preparation and characterization of chiral copper 12-metallacrown-4 complexes, inorganic analogues of tetraphenylporphyrinatocopper(II), Inorg. Chem. 37 (1998) 5416–5417.

[332] M. Branden, H. Sigurdson, A. Namslauer, R.B. Gennis, P. Adelroth, P. Brzezinski, On the role of the K-proton transfer pathway in cytochrome c oxidase, Proc. Natl. Acad. Sci. U. S. A. 98 (2001) 5013–5018.

[333] M.A. Sharpe, S. Ferguson-Miller, A chemically explicit model for the mechanism of proton pumping in heme-copper oxidases, J. Bioenerg. Biomembr. 40 (2008) 541–549.

[334] J. Liu, L. Qin, S. Ferguson-Miller, Crystallographic and online spectral evidence for role of conformational change and conserved water in cytochrome oxidase proton pump, Proc. Natl. Acad. Sci. U. S. A. 108 (2011) 1284–1289.

[335] D.A. Mills, L. Florens, C. Hiser, J. Qian, S. Ferguson-Miller, Where is 'outside' in cytochrome c oxidase and how and when do protons get there? Biochim. Biophys. Acta 1458 (2000) 180–187.

[336] R. Sugitani, E.S. Medvedev, A.A. Stuchebrukhov, Theoretical and computational analysis of the membrane potential generated by cytochrome c oxidase upon single electron injection into the enzyme, Biochim. Biophys. Acta 1777 (2008) 1129–1139.

[337] A.V. Pisliakov, P.K. Sharma, Z.T. Chu, M. Haranczyk, A. Warshel, Electrostatic basis for the unidirectionality of the primary proton transfer in cytochrome c oxidase, Proc. Natl. Acad. Sci. U. S. A. 105 (2008) 7726–7731.

[338] S. Chakrabarty, I. Namslauer, P. Brzezinski, A. Warshel, Exploration of the cytochrome c oxidase pathway puzzle and examination of the origin of elusive mutational effects, Biochim. Biophys. Acta 1807 (2011) 413–426.

[339] N. Ghosh, X. Prat-Resina, M.R. Gunner, Q. Cui, Microscopic pK$_a$ analysis of Glu286 in cytochrome c oxidase (Rhodobacter sphaeroides): toward a calibrated molecular model, Biochemistry 48 (2009) 2468–2485.

[340] J. Xu, G.A. Voth, Free energy profiles for H$^+$ conduction in the D-pathway of cytochrome c oxidase: a study of the wild type and N98D mutant enzymes, Biochim. Biophys. Acta 1757 (2006) 852–859.

[341] J. Xu, G.A. Voth, Redox-coupled proton pumping in cytochrome c oxidase: further insights from computer simulation, Biochim. Biophys. Acta 1777 (2008) 196–201.

[342] T. Yamashita, G.A. Voth, Insights into the mechanism of proton transport in cytochrome c oxidase, J. Am. Chem. Soc. 134 (2012) 1147–1152.

[343] M. Olsson, P. Siegbahn, M. Blomberg, A. Warshel, Exploring pathways and barriers for coupled ET/PT in cytochrome c oxidase: a general framework for examining energetics and mechanistic alternatives, Biochim. Biophys. Acta 1767 (2007) 244–260.

[344] M.H.M. Olsson, A. Warshel, Monte Carlo simulations of proton pumps: on the working principles of the biological valve that controls proton pumping in cytochrome c oxidase, Proc. Natl. Acad. Sci. 103 (2006) 6500–6505.

[345] Y.C. Kim, G. Hummer, Proton-pumping mechanism of cytochrome c oxidase: a kinetic master-equation approach, Biochim. Biophys. Acta 1817 (2012) 526–536.

[346] Y.C. Kim, M. Wikstrom, G. Hummer, Kinetic models of redox-coupled proton pumping, Proc. Natl. Acad. Sci. U. S. A. 104 (2007) 2169–2174.

[347] S. Yang, Q. Cui, Glu-286 rotation and water wire reorientation are unlikely the gating elements for proton pumping in cytochrome c oxidase, Biophys. J. 101 (2011) 61–69.

[348] V.R. Kaila, V. Sharma, M. Wikstrom, The identity of the transient proton loading site of the proton-pumping mechanism of cytochrome c oxidase, Biochim. Biophys. Acta 1807 (2011) 80–84.

[349] P.E. Siegbahn, M.R. Blomberg, Proton pumping mechanism in cytochrome c oxidase, J. Phys. Chem. A 112 (2008) 12772–12780.

[350] B. Durham, F. Millett, Design of photoactive ruthenium complexes to study electron transfer and proton pumping in cytochrome oxidase, Biochim. Biophys. Acta 1817 (2012) 567–574.

[351] P. Adelroth, M. Ek, P. Brzezinski, Factors determining electron-transfer rates in cytochrome c oxidase: investigation of the oxygen reaction in the R. sphaeroides enzyme, Biochim. Biophys. Acta 1367 (1998) 107–117.

[352] P. Ådelroth, M. Karpeforsa, G. Gildersona, F.L. Tomsonc, R.B. Gennis, P. Brzezinski, Proton transfer from glutamate 286 determines the transition rates between oxygen intermediates in cytochrome c oxidase, Biochim. Biophys. Acta 1459 (2000) 533–539.

[353] M. Wikström, M.I. Verkhovsky, The D-channel of cytochrome oxidase: an alternative view, Biochim. Biophys. Acta 1807 (2011) 1273–1278.

[354] V.R. Kaila, M.I. Verkhovsky, G. Hummer, M. Wikström, Mechanism and energetics by which glutamic acid 242 prevents leaks in cytochrome c oxidase, Biochim. Biophys. Acta 1787 (2009) 1205–1214.

[355] V.R. Kaila, M. Verkhovsky, G. Hummer, M. Wikstrom, Prevention of leak in the proton pump of cytochrome c oxidase, Biochim. Biophys. Acta 1777 (2008) 890–892.

[356] V.R. Kaila, M.I. Verkhovsky, G. Hummer, M. Wikström, Glutamic acid 242 is a valve in the proton pump of cytochrome c oxidase, Proc. Natl. Acad. Sci. U. S. A. 105 (2008) 6255–6259.

[357] R. Pomes, G. Hummer, M. Wikstrom, Structure and dynamics of a proton shuttle in cytochrome c oxidase, Biochim. Biophys. Acta 1365 (1999) 255–260.

[358] J. Quenneville, D.M. Popovic, A.A. Stuchebrukhov, Combined DFT and electrostatics study of the proton pumping mechanism in cytochrome c oxidase, Biochim. Biophys. Acta 1757 (2006) 1035–1046.

sphaeroides blocks turnover with O$_2$ but not with H$_2$O$_2$, Biochemistry 37 (1998) 3062–3067.

[359] D.M. Popovic, A.A. Stuchebrukhov, Coupled electron and proton transfer reactions during the O → E transition in bovine cytochrome c oxidase, Biochim. Biophys. Acta 1817 (2012) 506–517.

[360] R.M. Henry, C.H. Yu, T. Rodinger, R. Pomes, Functional hydration and conformational gating of proton uptake in cytochrome c oxidase, J. Mol. Biol. 387 (2009) 1165–1185.

[361] R.M. Henry, D. Caplan, E. Fadda, R. Pomes, Molecular basis of proton uptake in single and double mutants of cytochrome c oxidase, J. Phys. Condens. Matter 23 (2011) 234102.

[362] S. Yoshikawa, K. Shinzawa-Itoh, R. Nakashima, R. Yaono, E. Yamashit, N. Inoue, M. Yao, M.J. Fei, C.P. Libeu, T. Mizushima, H. Yamaguchi, T. Tomizaki, T. Tsukihara, Redox-coupled crystal structural changes in bovine heart cytochrome c oxidase, Science (1998) 1723–1729.

[363] J. Quenneville, D.M. Popovic, A.A. Stuchebrukhov, Redox-dependent pK_a of Cu_B histidine ligand in cytochrome c oxidase, J. Phys. Chem. B 108 (2004) 18383–18389.

[364] V.R. Kaila, M.I. Verkhovsky, M. Wikström, Proton-coupled electron transfer in cytochrome oxidase, Chem. Rev. 110 (2010) 7062–7081.

[365] A.L. Johansson, S. Chakrabarty, C.L. Berthold, M. Hogbom, A. Warshel, P. Brzezinski, Proton-transport mechanisms in cytochrome c oxidase revealed by studies of kinetic isotope effects, Biochim. Biophys. Acta 1807 (2011) 1083–1094.

[366] M.R. Gunner, E. Alexov, E. Torres, S. Lipovaca, The importance of the protein in controlling the electrochemistry of heme metalloproteins: methods of calculation and analysis, J. Biol. Inorg. Chem. 2 (1997) 126–134.